ENGINEERING RESEARCH INSTITUTE
DEPARTMENT OF AERONAUTICAL ENGINEERING
UNIVERSITY OF MICHIGAN
ANN ARBOR

APPLICATION OF DIFFERENCE TECHNIQUES TO THE LATERAL VIBRATION OF BEAMS USING THE ELECTRONIC DIFFERENTIAL ANALYZER

by

C. E. Howe

Professor of Physics,
Oberlin College

and

R. M. Howe

Assistant Professor of Aeronautical Engineering
University of Michigan

Project 2115

Office of Ordnance Research, U. S. Army
Contract No. DA-20-018-ORD-21811

AIR-7 February, 1954

PREFACE

This report describes some basic research on the application of difference techniques to the solution of the lateral vibration of beams. Time is in all cases preserved as a continuous variable; but distance along the beam is divided into stations, and derivatives with respect to that distance are approxmated by finite differences. Solution accuracies using the resulting equations are obtained both theoretically and by using the electronic differential analyzer. Similar equations have been solved by the Caltech electric analog computer,[15] which employs mainly passive circuit elements instead of operational-type feedback amplifiers. The passive-circuit computer has the advantage of simplicity, with the result that more complicated problems may be treated with a given size of installation. The active-circuit computer (electronic differential analyzer) has the advantage of a more flexible time-scale, higher accuracy, and ability to handle most types of nonlinearities.

In the present report we shall consider theoretically and with computer the lateral vibration of cantilever, free-free, hinged-hinged and clamped-clamped beams, both uniform and nonuniform. Time-varying boundary conditions, effects of transverse shear, and viscous damping will also be considered. Beam response to arbitrary forcing functions along the beam is demonstrated. In each case the directly-recorded outputs of the electronic differential analyzer are beam displacement, beam velocity, and bending moment as a function of time at various stations along the beam.

Beam equations with nonlinear terms such as velocity-squared damping have been solved and will be presented in a later report. Other reports will be issued describing the work which we have done on linear and non-linear heat-transfer problems, the solution of plate-vibration problems, and the solution of aeroelastic problems such as the gust response of aircraft wings.

The computer solutions were obtained with one of the electronic-differential analyzer installations in the Department of Aeronautical Engineering, University of Michigan. The computer used includes 80 drift-stabilized

---

15 Numbered superscripts refer to similarly numbered references in the bibliography at the end of this report.

operational amplifiers which are essentially similar to those discussed in another report.[12] Solutions were recorded on a Brush, Model BL-202 Oscillograph, a Sandborn Model 60-1300 Galvenometer, and a Reeves Mod 2 IO-101(A) Input-Output Table.

TABLE OF CONTENTS

TABLE OF CONTENTS (continued)

ILLUSTRATIONS

ILLUSTRATIONS (continued)

CHAPTER 1

INTRODUCTION

One problem which is often encountered in structural dynamics is that of the flexural vibrations of beams. For example, the transverse vibrations of an aircraft wing can be considered as a problem of this type. The equation describing this motion is a partial differential equation of fourth order in distance along the beam and second order in time. Solution of the equation by hand techniques for all but the simplest cases involving uniform beams is extremely tedious, and therefore an automatic computing device is clearly of considerable usefulness in this application.

The electronic differential analyzer is at present one of the most widely used types of computers for engineering problems. It is, however, limited to the solution of ordinary differential equations, since it can integrate with respect to only one variable, namely time. In order to solve the equation describing the problem of flexural vibration of beams, it is necessary to convert the partial differential equation to ordinary differential equations. If the problem is linear and the boundary conditions are suitable, the technique of separation of variables can be used to obtain eigenvalue-type equations. The differential analyzer is a convenient tool to solve for the eigenvalues and normal-mode solutions of these equations.[1-5] In Section 1.2 an example of the separation-of-variables technique is given.

On the other hand, if the original beam equations are nonlinear, e.g., include velocity-squared damping terms, nonlinear stress-strain relationships, etc., they cannot be handled by separation of variables. However, by considering the transverse displacement only at discrete stations along the beam, and by approximating spacial derivatives by finite differences, the original nonlinear partial differential equations can be rewritten as a system of ordinary nonlinear differential equations which can be solved by the electronic differential analyzer. Indeed, even when the equations are linear the difference method of analyzer solution, though in general somewhat less accurate than the eigenvalue approach, is much faster, more direct, and more versatile, allowing the introduction of time-dependent boundary conditions, arbitrary forcing functions, non-uniform characteristics along the beam,

viscous damping, etc.[6,7]

This report is a description of research on the application of difference techniques to the flexural-vibration problem. Before considering the theory of the difference method let us write down the beam equations.

1.1 Basic Equations for a Thin Beam

The elementary equation describing the dynamic transverse displacement y of a beam is given by[8]

$$\frac{\partial^2}{\partial \bar{x}^2} EI(\bar{x}) \frac{\partial^2 y(\bar{x}, \bar{t})}{\partial \bar{x}^2} + \rho(\bar{x}) \frac{\partial^2 y(\bar{x}, \bar{t})}{\partial \bar{t}^2} = \bar{f}(\bar{x}, \bar{t}) \qquad (1\text{-}1)$$

where $\bar{x}$ is distance along the beam, $\bar{t}$ is time, $EI(\bar{x})$ is the flexural rigidity at $\bar{x}$, $\rho(\bar{x})$ is the mass per unit length at $\bar{x}$, and $f(\bar{x}, \bar{t})$ is the external force per unit length applied along the beam. We recall that the bending moment $M(\bar{x}, \bar{t})$ is given by

$$M(\bar{x}, \bar{t}) = EI(\bar{x}) \frac{\partial^2 y(\bar{x}, \bar{t})}{\partial \bar{x}^2} \qquad (1\text{-}2)$$

and the shear force $V(\bar{x}, \bar{t})$ is given by

$$V(\bar{x}, \bar{t}) = \frac{\partial M(\bar{x}, \bar{t})}{\partial \bar{x}} \qquad (1\text{-}3)$$

Equation (1-1) is of course subject to boundary conditions which depend on the type of end fastening for the beam. For example the cantilever beam shown in Figure 1-1 has the following boundary conditions at the built-in end ($\bar{x} = 0$):

$$y(0, \bar{t}) = \frac{\partial y(0, t)}{\partial \bar{x}} = 0 \qquad (1\text{-}4)$$

i.e., at the built-in end the displacement and slope vanish. At the free end ($\bar{x} = L$) the conditions are

$$M(L, \bar{t}) = \frac{\partial M(L, \bar{t})}{\partial \bar{x}} = 0 \qquad (1\text{-}5)$$

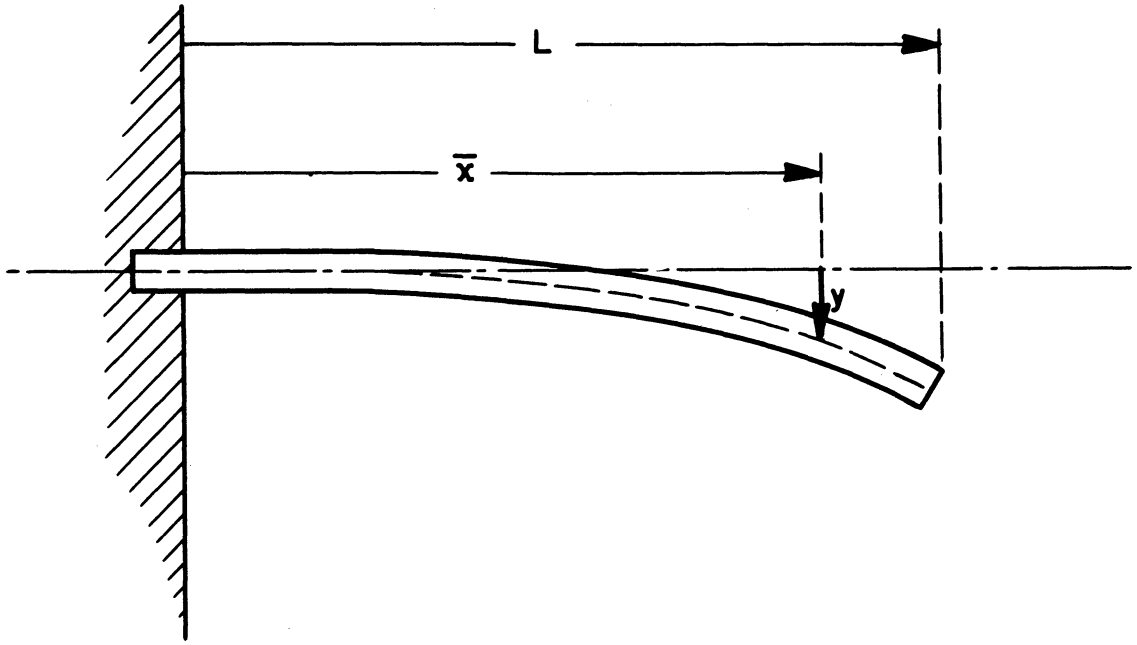

Figure 1-1 Cantilever Beam

i.e., at the free end the bending moment and shear force vanish. For a simply supported (hinged) end the displacement y and bending moment M must vanish.

In addition, initial conditions of the displacement and velocity along the beam must be specified. Thus let

$$y(\bar{x}, 0) = Y(\bar{x}) \tag{1-6}$$

$$\frac{\partial y(\bar{x}, 0)}{\partial \bar{t}} = Y(\bar{x}) \tag{1-7}$$

denote the initial conditions at $\bar{t} = 0$.

In writing Equation 1-1 a number of important assumptions have been made, including the assumption that the planes of flexure remain parallel and that the thickness of the beam is small compared with its length. This second assumption allows us to neglect the effect of rotary inertia and the deflection due to transverse shear force. In Chapter 10 the transverse shear force is included, and for thick beams the effect on the normal-mode frequencies is considerable.

Now that we have written the elementary beam equations it will be convenient to define a dimensionless distance variable x such that the beam length is unity in x. Thus let

$$x = \frac{\bar{x}}{L} \tag{1-8}$$

from which

$$\frac{\partial}{\partial \bar{x}} = \frac{\partial}{\partial x}\frac{dx}{d\bar{x}} = \frac{1}{L}\frac{\partial}{\partial x}; \quad \frac{\partial^2}{\partial \bar{x}^2} = \frac{1}{L^2}\frac{\partial^2}{\partial x^2}; \text{ etc.} \tag{1-9}$$

Also let us transform the variable characteristics of the flexural rigidity $EI(\bar{x})$ and mass per unit length $\rho(\bar{x})$ into dimensionless variables $\phi_f(\bar{x})$ and $\phi_d(\bar{x})$ respectively. Thus let

$$EI(\bar{x}) = EI_o\phi_f(\bar{x}) \tag{1-10}$$

and

$$\rho(\bar{x}) = \rho_o\phi_d(\bar{x}) . \tag{1-11}$$

Here EI_o and ρ_o are constants equal to the maximum value of $EI(\bar{x})$ and $\rho(\bar{x})$ respectively. For a uniform beam $\phi_f(\bar{x}) = \phi_d(\bar{x}) = 1$. From Equations (1-9), (1-10), and (1-11) the original beam equation (1-1) becomes

$$\frac{\partial^2}{\partial x^2}\phi_f(x)\frac{\partial^2 y(x,\bar{t})}{\partial x^2} + \frac{\rho_o L^4}{EI_o}\phi_d(x)\frac{\partial^2 y(x,\bar{t})}{\partial \bar{t}^2} = \frac{L^4}{EI_o}\bar{f}(x,\bar{t}) \tag{1-12}$$

Next we introduce a dimensionless time variable t given by

$$t = \frac{1}{L^2}\sqrt{\frac{EI_o}{\rho_o}}\,\bar{t} \tag{1-13}$$

from which

$$\frac{\partial^2}{\partial \bar{t}^2} = \frac{\partial^2}{\partial t^2}\left(\frac{dt}{d\bar{t}}\right)^2 = \frac{EI_o}{\rho_o L^4}\frac{\partial^2}{\partial t^2} \tag{1-14}$$

In terms of t Equation (1-12) becomes

$$\frac{\partial^2}{\partial x^2}\phi_f(x)\frac{\partial^2 y(x,t)}{\partial x^2} + \phi_d(x)\frac{\partial^2 y(x,t)}{\partial t^2} = f(x,t) \qquad (1\text{-}15)$$

where

$$f(x,t) = \frac{L^4}{EI_o}\tilde{f}(x,t) \qquad (1\text{-}16)$$

For a cantilever beam the boundary conditions become

$$y(0,t) = \frac{\partial y(0,t)}{\partial x} = 0 \qquad (1\text{-}17)$$

$$M(1,t) = \frac{\partial M(1,t)}{\partial x} = 0 \qquad (1\text{-}18)$$

Equation (1-15) is the linear equation which we will solve in this report with the differential analyzer.

1.2 Solution by Separation of Variables

Before introducing the difference method for converting Equation (1-15) into a system of ordinary differential equations, let us review the separation-of-variables method for solving the beam equation. Consider the case where $f(x,t) = 0$. Assume that the displacement $y(x,t)$ can be written as

$$y(x,t) = X(x)T(t) \qquad (1\text{-}19)$$

Substituting Equation (1-19) into Equation (1-15), we have

$$T(t)\frac{d^2}{dx^2}\phi_f(x)\frac{d^2X(x)}{dx^2} + \phi_d(x)X(x)\frac{d^2T(t)}{dt^2} = 0 \qquad (1\text{-}20)$$

or

$$\frac{1}{\phi_d(x)X(x)}\frac{d^2}{dx^2}\phi_f(x)\frac{d^2X(x)}{dx^2} = -\frac{1}{T(t)}\frac{d^2T(t)}{dt^2} \qquad (1\text{-}21)$$

Since the left side of Equation (1-21) is a function only of x and the right side is a function only of t, the only way they can be equal for all x and t is for both sides to be equal to the same constant. Thus let

$$-\frac{1}{T(t)}\frac{d^2T(t)}{dt^2} = \beta^2$$

or

$$\frac{d^2T(t)}{dt^2} + \beta^2 T(t) = 0 \qquad (1\text{-}22)$$

In the same way

$$\frac{d^2}{dx^2}\phi_f(x)\frac{d^2X(x)}{dx^2} - \beta^2\phi_d(x)X(x) = 0 \qquad (1\text{-}23)$$

Evidently we have transformed the original partial differential equation (1-15) into two ordinary differential equations (1-22) and (1-23). The solution to Equation (1-22) is simple harmonic motion of frequency β, i.e.,

$$T(t) = A\cos\beta t \pm B\sin\beta t \qquad (1\text{-}24)$$

Equation (1-23) is subject to the boundary conditions of the original problem, since homogeneous boundary conditions on X(x) must also be met by y(x, t). For example, for a cantilever beam

$$X(0) = \frac{dX(0)}{dx} = 0 \qquad (1\text{-}25)$$

$$\phi_f(1)\frac{d^2X(1)}{dx^2} = \frac{d}{dx}\phi_f(1)\frac{d^2X(1)}{dx^2} = 0 \qquad (1\text{-}26)$$

It turns out that solutions X(x) to Equation (1-23) can satisfy the boundary conditions only for certain discrete values β_n of the constant β. The solution $X_1(x)$ corresponding to the smallest allowable value β_1 gives the magnitude along the beam of the lowest mode of sinusoidal oscillation. $X_2(x)$ gives the shape of the second mode, which oscillates at the frequency β_2, etc. The discrete values β_n of β are known as eigenvalues, and the corresponding solutions $X_n(x)$ are called normal modes.

One can show that any arbitrary beam motion y(x, t) can be represented by the proper combination of the normal-modes. Thus

$$y(x,t) = \sum_{n=1}^{\infty} X_n(x)(A_n \cos \beta_n t + B_n \sin \beta_n t) \tag{1-27}$$

The initial conditions given by Equation (1-6) and (1-7) along with the orthogonality properties of $X_n(x)$, are used to evaluate the coefficients A_n and B_n in Equation (1-27). Thus for built-in, hinged, or free end conditions one can show from Equation (1-23) that

$$\int_0^1 \phi_d(x) X_n(x) X_m(x) dx = 0, \quad n \neq m \tag{1-28}$$

$$= N_n, \quad n = m$$

As an example assume that the initial velocity $\frac{\partial y(x,0)}{\partial t} = \dot{Y}(x)$, and that $y(x,0) = Y(x)$. At $t = 0$ Equation (1-27) becomes

$$Y(x) = \sum_{n=1}^{\infty} A_n X_n(x) \tag{1-29}$$

Multiplying both sides of Equation (1-29) by $\phi_d(x) X_m(x)$ and integrating from $x = 0$, to $x = 1$, we have

$$\int_0^1 \phi_d(x) Y(x) X_m(x) dx = \sum_{n=1}^{\infty} A_n \int_0^1 \phi_d(x) X_n(x) X_m(x) dx \tag{1-30}$$

From the orthogonality relationship in Equation (1-28) it is clear that all the terms on the right side of Equation (1-30) are zero except the one for which $n = m$, where the right side is $A_n N_n$. The solution for A_n is then

$$A_n = \frac{1}{N_n} \int_0^1 \phi_d(x) Y(x) X_n(x) dx \tag{1-31}$$

In the same way

$$B_n = \frac{1}{\beta_n N_n} \int_0^1 \phi_d(x) \dot{Y}(x) X_n(x) dx \tag{1-32}$$

The method for calculating the complete solution to the beam equation using separation of variables is apparent. First the normal mode frequencies β_n and the accompanying normal-mode functions $X_n(x)$ must be computed, along with the normalizing constants N_n defined in Equation (1-28). Next the coefficients A_n and B_n are calculated from Equations (1-31) and (1-32). Finally, the complete solution is obtained by summing the contributions of all the normal modes, as indicated in Equation (1-27). Although in theory an infinite number of modes is required to build up the arbitrary initial conditions, in practice only the first several modes are needed to give a reasonably accurate representation, providing the initial condition functions $Y(x)$ and $Y(x)$ are fairly well behaved.

The electronic differential analyzer can be used to solve the eigenvalue Equation (1-23) and to compute the coefficients A_n and B_n in Equations (1-31) and Equation (1-32). In Chapter 3 we will consider the normal-mode solution to Equation (1-23) for uniform beams ($\phi_f = \phi_d = 1$) in order to compare the results with the difference method.

1.3 Replacement of Partial Derivatives by Finite Differences

We have already seen in Section 1.1 that the equation for transverse vibration of a beam is a partial differential equation, fourth order in distance x along the beam, second order in time t. Hence the beam displacement $y(x, t)$ is a function both of the dimensionless distance variable x and the dimensionless time variable t. Instead of measuring y at all distances x, let us measure y only at discrete stations along x, as shown in Figure 1-2; thus let y_1 be the beam displacement at the first x station, y_2 be the displacement at the second x station, y_n be the displacement at the nth x station. Further, let the distance between stations be a constant Δx.

Now clearly a good approximation to $\partial y / \partial x\big|_{\frac{1}{2}}$ (i.e., the partial derivative of y with respect to x at the 1/2 station) is given by the difference

$$\left.\frac{\partial y}{\partial x}\right|_{\frac{1}{2}} = \frac{y_1 - y_o}{\Delta x} \qquad (1\text{-}33)$$

In fact the limit of Equation (1-33) as $\Delta x \to 0$ is just the definition of the partial derivative with respect to x at $x = \frac{1}{2}(\Delta x)$. Writing Equation

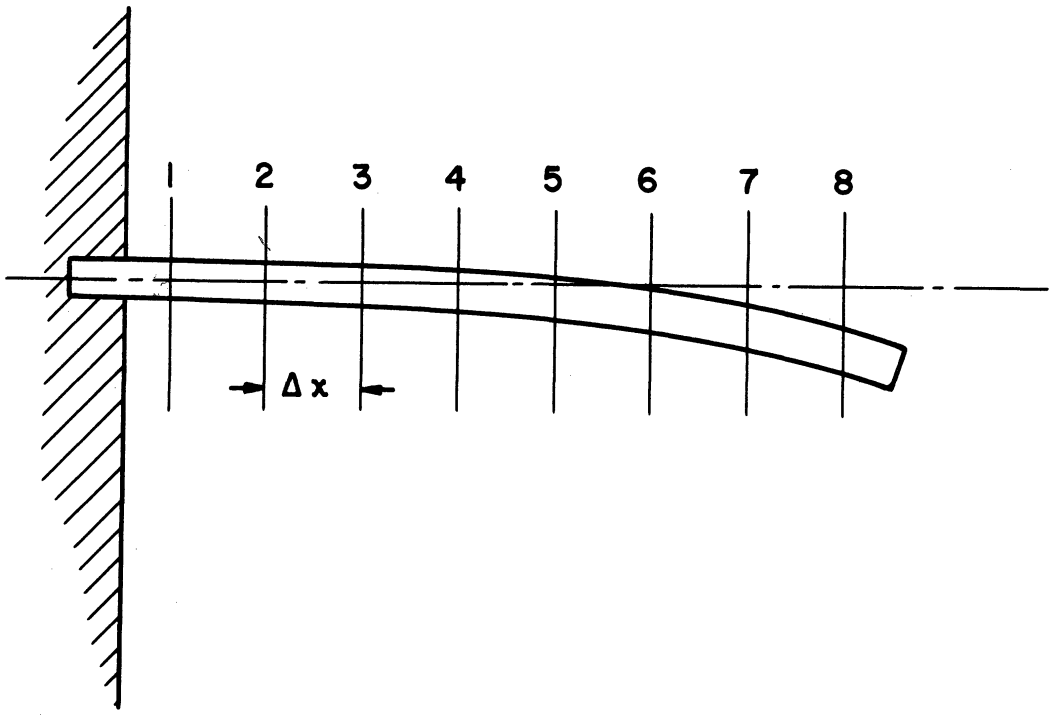

Figure 1-2 Station Arrangement for Cantilever Beam

(1-33) in more general terms, we have

$$\left.\frac{\partial y}{\partial x}\right|_{n-\frac{1}{2}} = \frac{y_n - y_{n-1}}{\Delta x} \tag{1-34}$$

In the same way

$$\left.\frac{\partial^2 y}{\partial x^2}\right|_n = \frac{1}{\Delta x}\left[\left.\frac{\partial y}{\partial x}\right|_{n+\frac{1}{2}} - \left.\frac{\partial y}{\partial x}\right|_{n-\frac{1}{2}}\right] \tag{1-35}$$

or from Equation (1-34)

$$\left.\frac{\partial^2 y}{\partial x^2}\right|_n = \frac{y_{n-1} - 2y_n + y_{n-1}}{(\Delta x)^2} \tag{1-36}$$

Similar approximations can be written for higher derivatives.

Evidently we have replaced partial derivatives of y with respect to x by algebraic differences. The only rates of change of the variables y_1, y_2, ... y_n, . . . are with respect to the time variable t, so that we are left with a system of ordinary differential equations involving dependent variables

$y_o(t)$, $y_1(t)$ . . . $y_n(t)$. This difference method can of course be used in general to rewrite a partial differential equation as a system of ordinary differential equations.[6,7] The specific equations obtained for the case of transverse beam vibration are discussed in the next section.

CHAPTER 2

DERIVATION OF THE DIFFERENCE EQUATION FOR BEAMS

2.1 Equation for the n-th Cell

In Section 1.1 we saw that the equation for transverse displacement y of a beam could be written as

$$\frac{\partial^2}{\partial x^2}\phi_f(x)\,\frac{\partial^2 y(x,t)}{\partial x^2} + \phi_d(x)\,\frac{\partial^2 y(x,t)}{\partial t^2} = f(x,t) \qquad (1\text{-}15)$$

where x is dimensionless distance along the beam defined in Equation (1-8), t is dimensionless time defined in Equation (1-13), and where $\phi_f(x)$ and $\phi_d(x)$ are defined in Equation (1-10) and (1-11) as representing the variation along the beam of flexural rigidity and mass per unit length respectively. From Equations (1-2), (1-8) and (1-10) the bending moment M(x, t) is given by

$$M(x,t) = \frac{EI_o}{L^2}\phi_f(x)\,\frac{\partial^2 y(x,t)}{\partial x^2} \qquad (2\text{-}1)$$

and from Equations (1-3) and (1-8) the shear force V(x, t) is given by

$$V(x,t) = \frac{1}{L}\,\frac{\partial M(x,t)}{\partial x} \qquad (2\text{-}2)$$

Following the procedure introduced in Section 1.3, we will consider the displacement y only at certain stations in x, with distance between stations given by Δx. It is convenient to introduce still a third distance variable χ such that the distance $\Delta\chi$ between χ stations is unity. If the entire beam were divided into N stations, then

$$\chi = Nx \qquad (2\text{-}3)$$

and the beam length in the new χ variable is simply N. Equation (1-15), written in terms of χ, becomes

$$\frac{\partial^2}{\partial\chi^2}\phi_f(\chi)\,\frac{\partial^2 y(\chi,t)}{\partial\chi^2} + \phi_d(\chi)\,\frac{\partial^2 y(\chi,t)}{\partial(N^2t)^2} = \frac{1}{N^4}f(\chi,t) \qquad (2\text{-}4)$$

If we now introduce another time variable τ given by

$$\tau = N^2 t \tag{2-5}$$

and a force variable $\Phi(\chi, t)$ given by

$$\Phi(\chi, t) = \frac{1}{N^4} f(\chi, t) \tag{2-6}$$

Equation (2-4) becomes

$$\frac{\partial^2}{\partial \chi^2}\phi_f(\chi)\frac{\partial^2 y(\chi,\tau)}{\partial \chi^2} + \phi_d(\chi)\frac{\partial^2 y(\chi,\tau)}{\partial \tau^2} = \Phi(\chi,\tau) \tag{2-7}$$

where the distance between stations $\Delta\chi = 1$, and where the beam length = N if the beam is divided into N segments. From Equations (1-36), (2-1), and (2-3) the bending moment M_n at the n-th station can be written approximately as

$$M_n = \frac{N^2}{L^2} EI_o \phi_{f_n} (y_{n+1} - 2y_n + y_{n-1}) \tag{2-8}$$

If we let m_n be proportional to the actual bending moment M_n and given by

$$m_n = \frac{L^2}{N^2 EI_o} M_n \tag{2-9}$$

then

$$m_n = \phi_{f_n} (y_{n+1} - 2y_n + y_{n-1}) \tag{2-10}$$

Hereafter we will refer to m_n as the bending moment at station n. even though it is understood that m_n must be multiplied by L^2/N^2EI_o to obtain the actual bending moment M_n.

From Equations (1-36) and (2-7) it is clear that the dynamic equation for the displacement y_n at the n-th χ station becomes

$$\phi_{d_n}\frac{d^2 y_n}{d\tau^2} = -m_{n+1} + 2m_n - m_{n-1} + \Phi_n(\tau) \tag{2-11}$$

For our N - station beam Equation (2-6) would be iterated N times, so that a system of simultaneous ordinary differential equation must now be solved.

2.2 Boundary Conditions

The type of end fastenings for the beam will determine the boundary conditions. The boundary conditions for the cantilever beam shown in Figure 1-1 are summarized in Equation (1-4) and (1-5). At the built-in end the displacement and slope both vanish. Let us consider what these conditions imply for displacements at the stations of the cellular beam. Assume that the left end of the beam occurs at station 1/2, and the slope $\partial y / \partial \chi \Big|_{1/2}$ vanishes at that point. The condition that the displacement also vanishes implies that $y_o = y_1 = 0$.

At the free end the bending moment and shear force vanish. Assuming that the free end occurs at station $N + 1/2$, and the shear force $\partial M/\partial \chi \Big|_{N+\frac{1}{2}}$ at that station must vanish. This, in addition to the zero bending-moment condition, implies that the free-end $m_N = m_{N+1} = 0$. The complete difference equations for the cantilever beam with built-in end at $\chi = 1/2$, free end at $\chi = N + 1/2$, are from Equation (2-10) and (2-11)

$$\phi_{d_2} \frac{d^2 y_2}{d\tau^2} = - m_3 + 2m_2 - m_1 + \Phi_2(\tau)$$

$$\phi_{d_3} \frac{d^3 y_3}{d\tau^2} = m_4 + 2m_3 - m_2 + \Phi_3(\tau) \qquad (2\text{-}12)$$

$$\phi_{d_{N-2}} \frac{d^2 y_{N-2}}{d\tau^2} = - m_{N-1} + 2m_{N-2} - m_{N-3} + \Phi_{N-2}(\tau)$$

$$\phi_{d_{N-1}} \frac{d^2 y_{N-1}}{d\tau^2} = 2m_{N-1} - m_{N-2} + \Phi_{N-1}(\tau)$$

$$\phi_{d_N} \frac{d^2 y_N}{d\tau^2} = - m_{N-1} + \Phi_N(\tau)$$

where the bending moments are given by

$$m_1 = \phi_{f_1} y_2$$

$$
\begin{aligned}
m_2 &= \phi_{f_2}(y_3 - 2y_2) \\
m_3 &= \phi_{f_3}(y_4 - 2y_3 + y_2) \\
m_4 &= \phi_{f_4}(y_5 - 2y_4 + y_3) \\
&\cdot \quad \cdot \quad \cdot \quad \cdot \\
&\cdot \quad \cdot \quad \cdot \quad \cdot \\
m_{N-1} &= \phi_{f_{N-1}}(y_N - 2y_{N-1} + y_{N-2})
\end{aligned}
\tag{2-13}
$$

Equations (2-12) and (2-13) are a set of N-1 simultaneous second-order ordinary differential equations. The cantilever beam they represent for N = 8 (8-cells) is shown schematically in Figure 1-2. Note that although the end actually occurs at $\chi = 1/2$, the displacement y_1 at $\chi = 1$ is equal to zero.

For a hinged end the displacement and bending moment vanish. For a hinged end at $\chi = 0$, $y_o = 0$ and $M_o = 0$ satisfy this condition. The following table summarizes the boundary conditions for the various kinds of end fastenings when the difference approximation is made.

TABLE I

Summary of Boundary Conditions for Difference Method

Type of End Fastenings	Where End Occurs	Condition
Built-In	$N + \frac{1}{2}$	$y_N = y_{N+1} = 0$
Free	$N + \frac{1}{2}$	$m_N = m_{N+1} = 0$
Hinged	N	$y_N = m_N = 0$

Thus far we have considered only fixed homogeneous boundary conditions. Actually, time dependent boundary conditions can be included in the equations. An example of this type is considered in Section 9.1.

2.3 Initial Conditions

Finally, to complete the formulation of the difference-method approximation to the beam equation we should point out that initial displacement and velocity conditions must be specified to solve the problem. The original initial conditions at $\tau = 0$ given by Equations (1-6) and (1-7) are

$$y(X, 0) = Y(X)$$

and

$$\frac{\partial y(X, 0)}{\partial \tau} = \frac{N^2}{L^2}\sqrt{\frac{EI_o}{\rho_o}}\, Y(X) \qquad (2\text{-}14)$$

when written as functions of X and τ. For the difference equations the conditions become simply

$$y_n(0) = Y_n$$

and

$$\frac{dy_n(0)}{d\tau} = \frac{N^2}{L^2}\sqrt{\frac{EI_o}{\rho_o}}\, Y_n \qquad (2\text{-}15)$$

We have now formulated completely the equations necessary to solve by difference techniques the partial differential equation representing the flexural vibrations of beams.

2.4 Summary of Variable Transformations

Because so may variable transformations were utilized to convert the original beam equation to suitable difference form, it would seem appropriate to review the changes of variables. Originally we started with the beam equation

$$\frac{\partial^2}{\partial \bar{x}^2} EI(\bar{x}) \frac{\partial^2 y(\bar{x}, \bar{t})}{\partial \bar{x}^2} + \rho(\bar{x}) \frac{\partial^2 y(\bar{x}, \bar{t})}{\bar{t}^2} = \bar{f}(\bar{x}, \bar{t}) \qquad (1\text{-}1)$$

for a beam of length L. By letting $x = \frac{\bar{x}}{L}$, $EI(x) = EI_o \phi_f(x)$, $\rho(x) = \rho_o \phi_d(x)$, $t = \frac{1}{L^2}\sqrt{\frac{EI_o}{\rho_o}}\,\bar{t}$, and $f(x,t) = \frac{L^4}{EI_o}\bar{f}(x,t)$, we obtained

$$\frac{\partial^2}{\partial x^2} \phi_f(x) \frac{\partial^2 y(x,t)}{\partial x^2} + \phi_d(x) \frac{\partial^2 y(x,t)}{\partial t^2} = f(x,t) \qquad (1\text{-}15)$$

for a beam of unit length.

Finally, when considering the beam only at stations in y we let $\chi = Nx$, $\tau = N^2 t$, and $\Phi = \frac{1}{N^4} f$, obtaining at the n-th cell

$$\phi_{d_n} \frac{d^2 y_n}{d\tau^2} = - m_{n+1} + 2m_n - m_{n-1} + \Phi_n(\tau) \qquad (2\text{-}11)$$

where

$$m_n = \phi_{f_n} (y_{n+1} - 2y_n + y_{n-1}) \qquad (2\text{-}10)$$

Here the distance $\Delta\chi$ between cells is unity, and an N-section beam has a length of N. Equations (2-10) and (2-11) are in a form convenient to set up on the electronic differential analyzer.

CHAPTER 3

ELECTRONIC DIFFERENTIAL ANALYZER CIRCUIT FOR SOLVING THE BEAM EQUATION BY THE DIFFERENCE METHOD

3.1 Linear Operations of the Electronic Differential Analyzer

For a more complete description of the theory of electronic differential analyzers the reader unfamiliar with this type of computer is directed to other references.[1,2,10] Here we will review briefly the principles of operation. The inputs and outputs to the electronic differential analyzer are voltages. The basic component of the computer is the operational amplifier, shown schematically in Figure 3-1a. It consists of a high-gain dc amplifier with feedback impedance Z_f and input impedance Z_i. By making the ratio Z_f/Z_i equal to a constant k, any input voltage e_1 can be multiplied by k to give an output voltage $e_o = -ke_1$. Note that a sign reversal is also obtained through the amplifier.

If more than one input impedance is used, as shown in Figure 3-1b, the operational amplifier can be used to sum several input voltages. Finally, if an input resistor R and feedback capacitor C are employed, as shown in Figure 3-1c, the output voltage is proportional to the time integral of the input voltage, the constant of proportionality being 1/RC.

By using the properties of multiplication by a constant, summation, sign-reversal, and time integration of voltages, the operational amplifiers can be connected to solve ordinary linear differential equations. By employing multipliers[10,11] nonlinear ordinary differential equations can be solved.

In order to apply initial conditions to the problem being solved on the analyzer, the feedback condensers on the integrating amplifiers are initially charged to the proper voltages by means of relay circuits.[10] When one disires the solution to begin, the initial condition relays are opened, releasing all the initial condition voltages which had been held on the integrating capacitors. The electronic differential analyzer then proceeds to generate the solution as time-varying output voltages. These can be recorded by any convenient device.

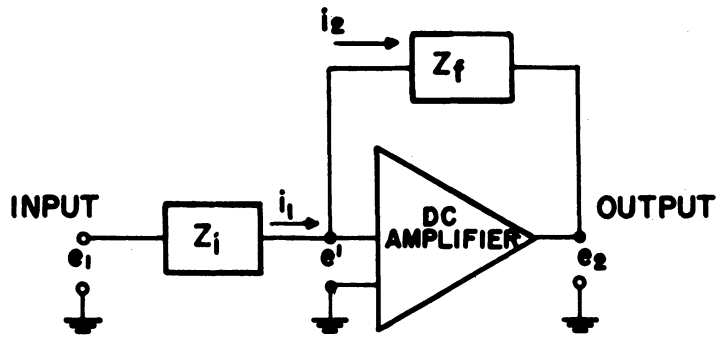

$$e_2 = -\frac{Z_f}{Z_i} e_1$$

a.) OPERATIONAL AMPLIFIER

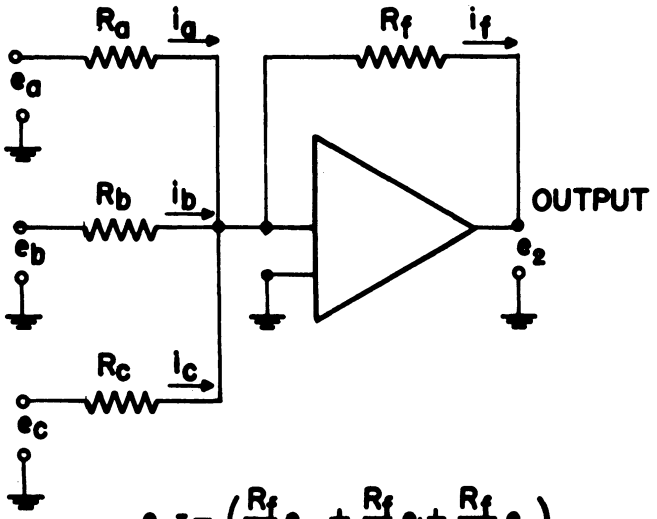

$$e_2 = -\left(\frac{R_f}{R_a} e_a + \frac{R_f}{R_b} e_b + \frac{R_f}{R_c} e_c\right)$$

b.) OPERATIONAL AMPLIFIER AS A SUMMER

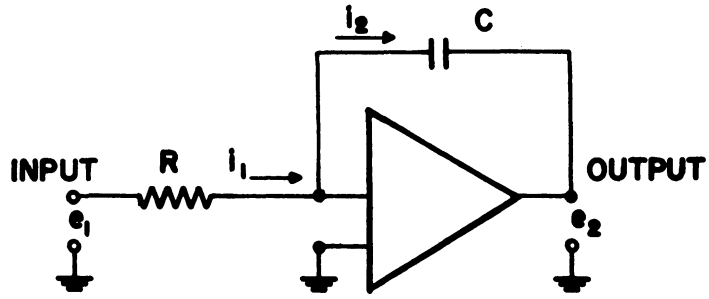

$$e_2 = -\frac{1}{RC}\int e_1 \, dt$$

C.) OPERATIONAL AMPLIFIER AS AN INTEGRATOR

Figure 3-1 Operational Amplifiers

3.2 Analyzer Circuit for a Cantilever Beam

The equations for solving the cantilever beam shown in Figure 1-2 by means of the difference technique are given by Equations (2-12) and (2-13). The electronic differential analyzer circuit which solves these equations for an N-cell beam is shown in Figure 3-2. The left end (built-in) occurs at the 1/2 station, whereas the right end (free) occurs at the N + 1/2 station. Ground connections and initial-conditions circuits are omitted for clarity. Note in the figure that single fixed resistors represent the flexural rigidity characteristic ϕ_{f_n} and mass constant ϕ_{d_n} respectively. The force Φ_n at each station is introduced as a time- varying voltage. Output voltages include the displacement, bending-moment, and velocity at each station as a function of time. Shear force and acceleration can be recorded at any station merely by using an additional amplifier to sum the proper voltages.

In Figure 3-2 the time constant of the integrators is RC seconds. The values of R and C selected for any particular problem determine the relationship between computer time τ and real time in seconds. For example, if we let C = 1 microfarad and R = 0.2 megohms, RC = 0.2 seconds and one unit of τ equals 0.2 seconds.

It is apparent from Figure 3-2 that for an N-cell cantilever beam, 3(N-1) operational amplifiers are required. Note that the output of every other row of amplifiers is reversed in sign, so that additional sign inverters do not have to be employed to compute the differences.

The computer circuit for an 8-cell uniform cantilever beam was set up on the electronic differential analyzer. An integrator time constant of 0.2 seconds was obtained with R = 0.2 megohms and C = 1 microfarad. Response curves following a one-second impulse applied equally at all stations are shown in Figure 3-3. Note the fundamental, long-period oscillation and the superimposed higher modes.

3.3 Analyzer Circuit for a Hinged-Hinged Beam

To illustrate the use of simply-supported or hinged end conditions we next consider the electronic differential analyzer circuit for solving a hinged-hinged beam by the difference technique (see Figure 3-4). The circuit

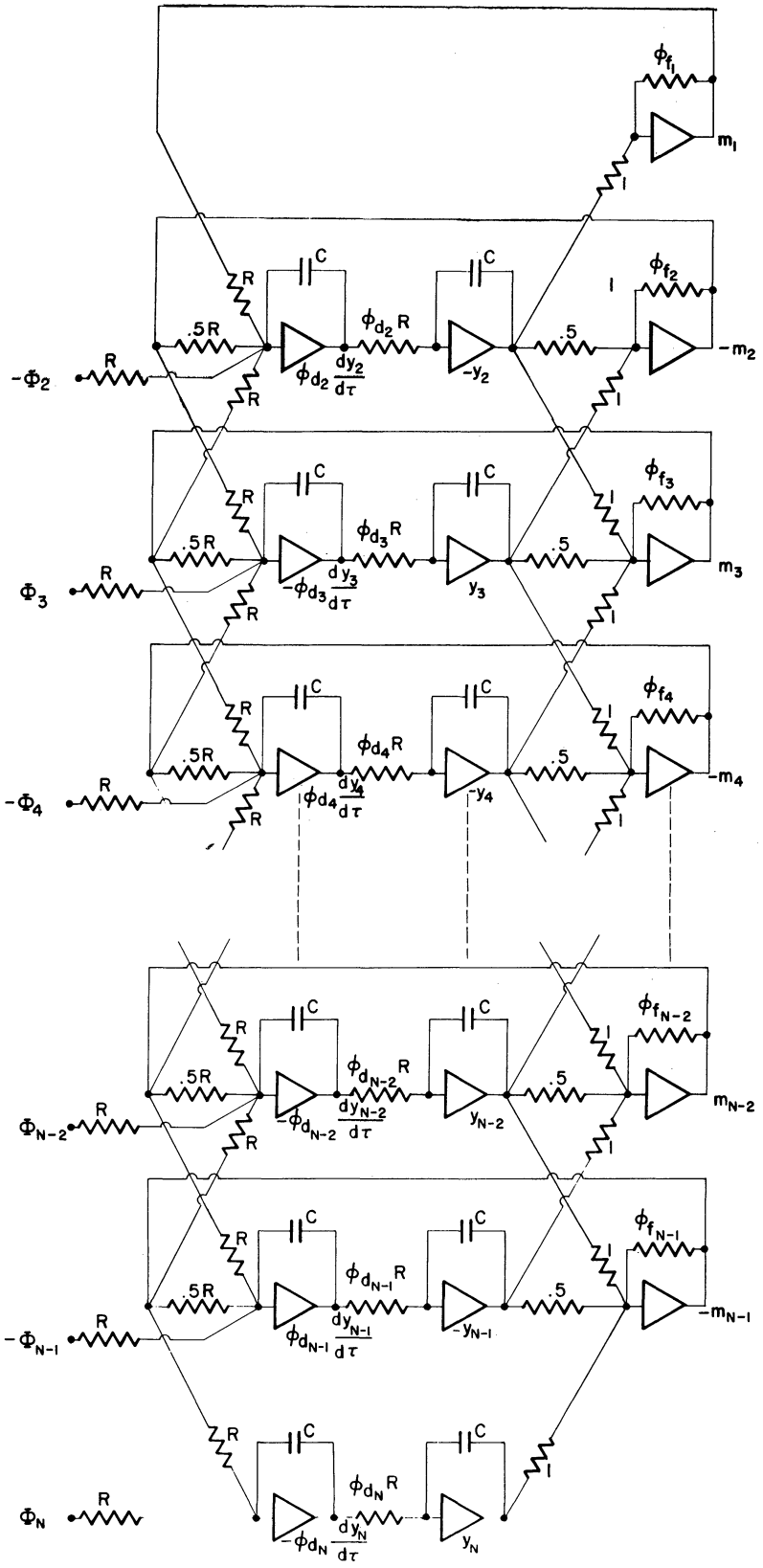

Figure 3-2 Analyzer Circuit for a Cantilever Beam

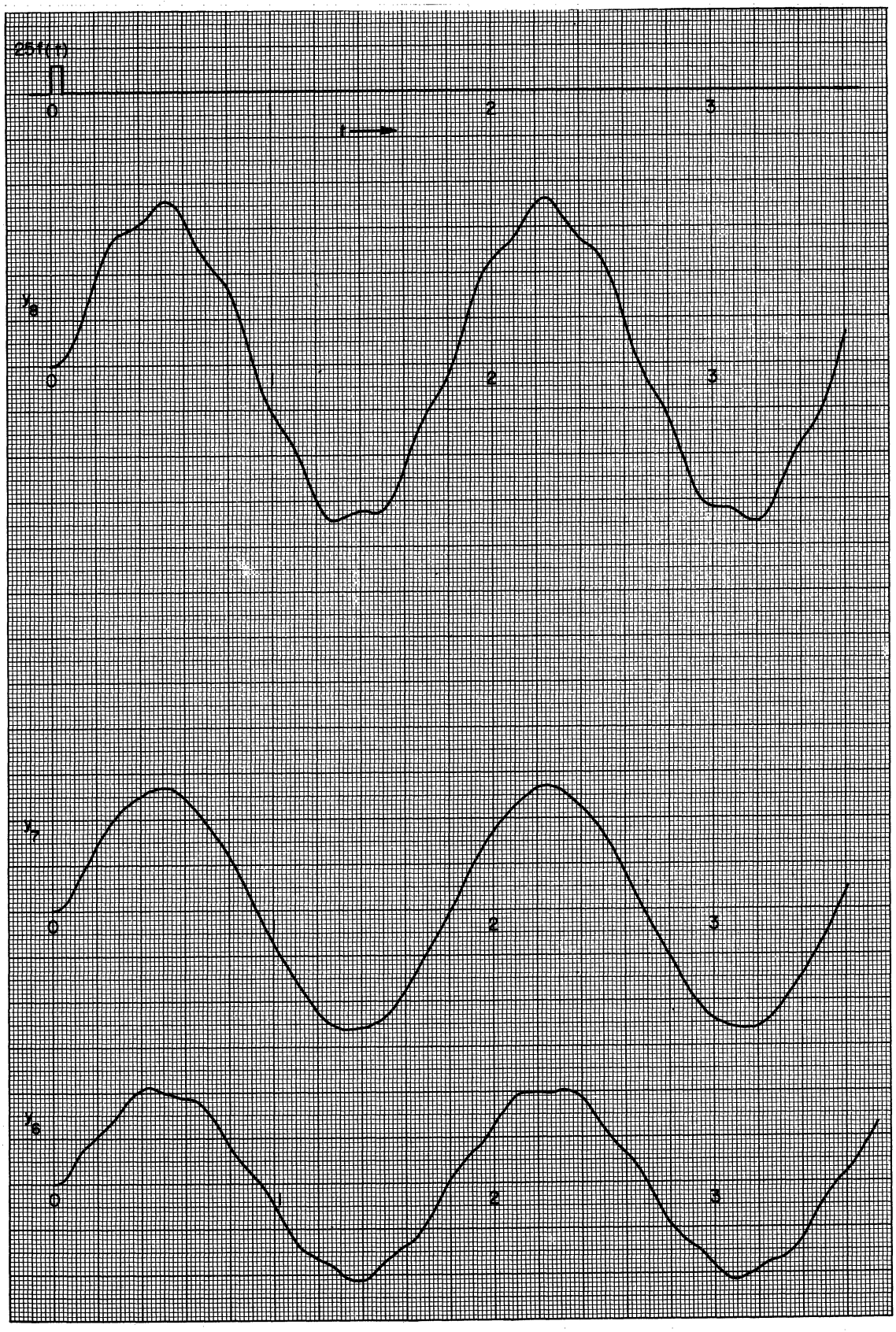

Figure 3-3a Response of 8-cell Uniform Cantilever Beam to a Uniform Impulse; Stations 6, 7, and 8

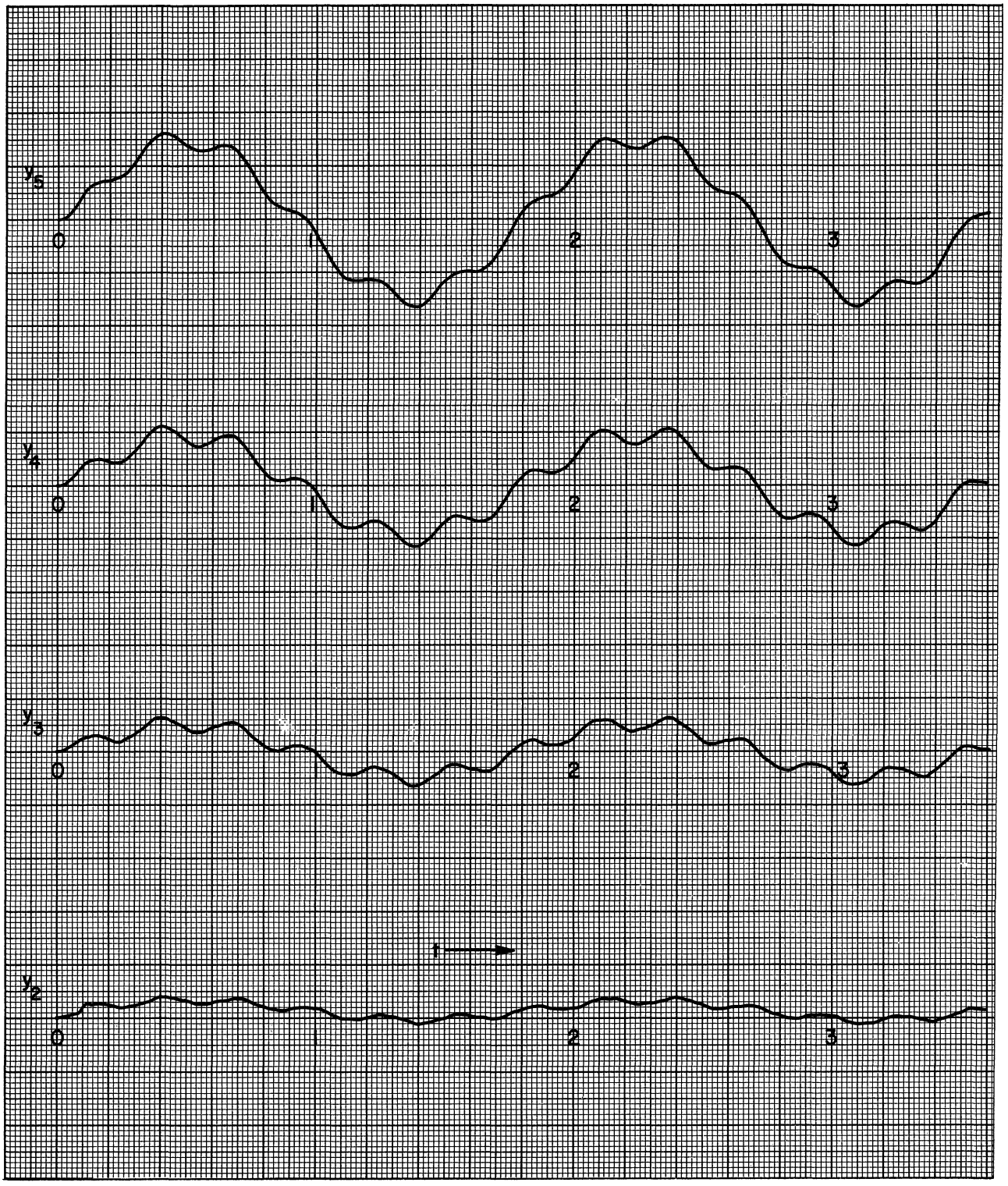

Figure 3-3b Response of 8-cell Uniform Cantilever Beam to a Uniform Impulse; Stations 2, 3, 4, and 5

is shown in Figure 3-5. It is similar to the circuit in Figure 3-2 for the cantilever beam except for the hinged ends, which occur at the zero station and N-th station for an N-cell beam. At the ends the displacement and bending moment vanish, so that $y_o = m_o = y_N = m_N = 0$. Again it is evident from the figure that an N-cell hinged-hinged beam, when solved by the difference technique, requires 3(N-1) operational amplifiers.

In later sections we will consider the circuits for introducing viscous damping into the beam equations.

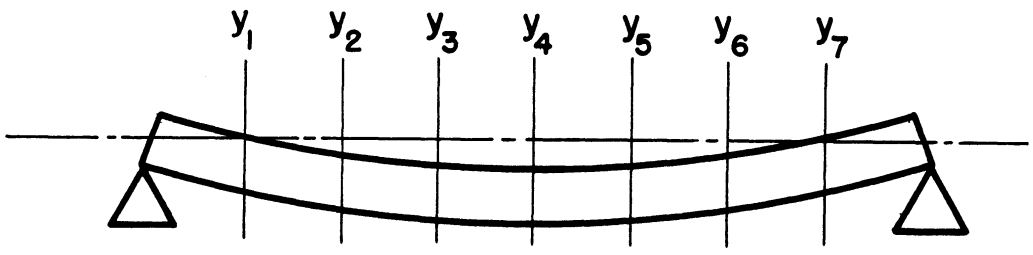

Figure 3-4 Hinged-Hinged Beam

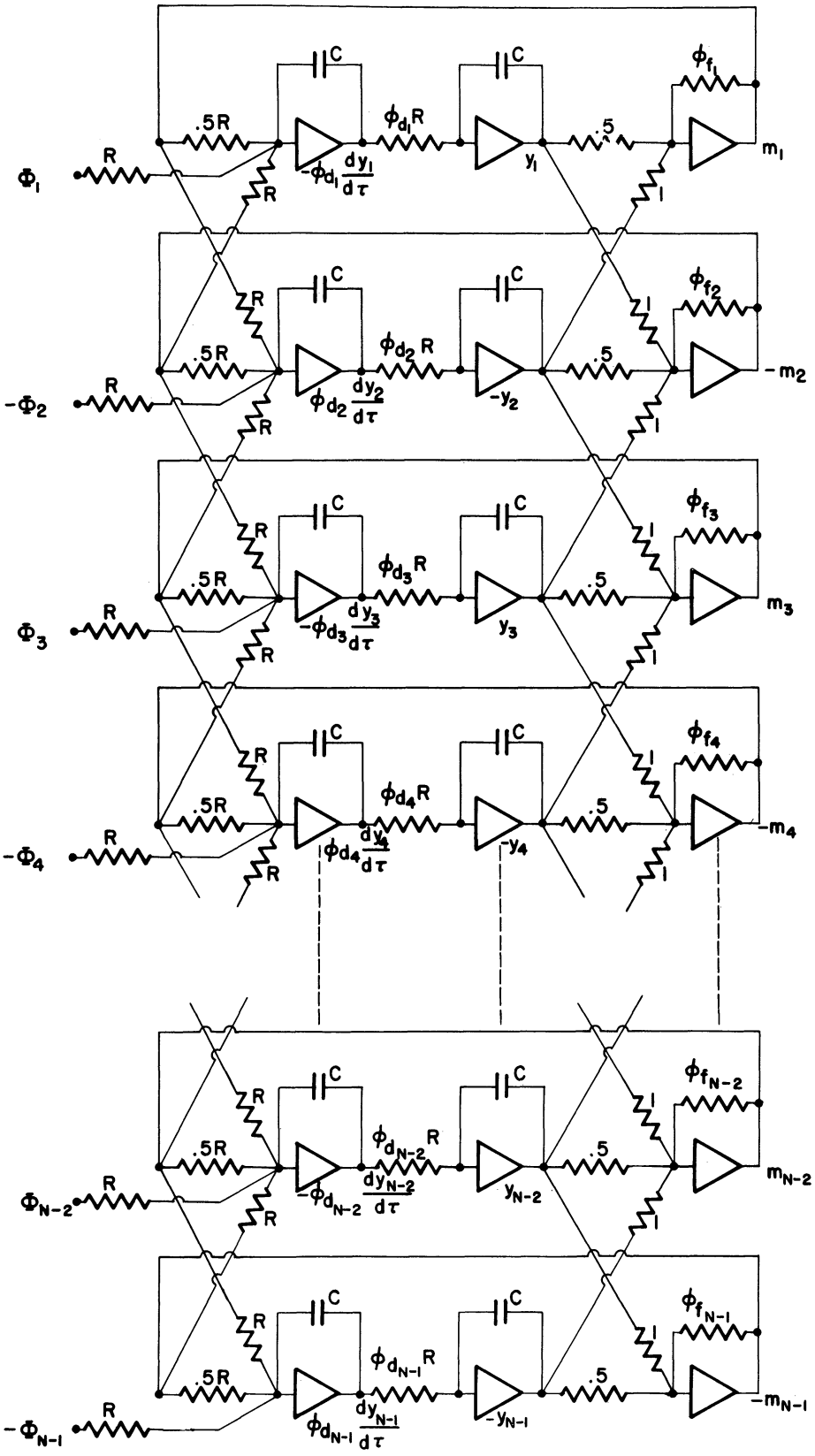

Figure 3-5 Analyzer Circuit for Hinged-Hinged Beam

CHAPTER 4

THEORETICAL ACCURACY OF THE DIFFERENCE TECHNIQUE FOR UNIFORM BEAMS

4.1 Uniform Hinged-Hinged Beam

Before we consider further examples of electronic differential analyzer solutions of the beam problem, let us estimate the accuracy of the difference technique. To do this we will calculate the frequencies and mode shapes obtained for sinusoidal normal-mode oscillations when the difference method is used. These frequencies and mode shapes will then be compared with theoretical ones for a continuous beam. If the frequencies and shapes show reasonable agreement, then we know that the difference-method will yield fairly accurate results in general, since any motion of the beam can be thought of as a super-position of the normal modes.

Because it is the simplest to treat mathematically, let us consider first the hinged-hinged or simply supported uniform beam. According to Equation (1-15) the equation describing the transverse vibrations for an unforced uniform beam is given by

$$\frac{\partial^4 y(x,t)}{\partial x^4} + \frac{\partial^2 y(x,t)}{\partial t^2} = 0 \qquad (4\text{-}1)$$

Here x is dimensionless distance along a beam of unit length, and t is a dimensionless time variable given by Equation (1-13). For a hinged-hinged beam the boundary conditions are

$$y(0,t) = \frac{\partial^2 y(0,t)}{\partial x^2} = y(1,t) = \frac{\partial^2 y(1,t)}{\partial x^2} = 0 \qquad (4\text{-}2)$$

Let us solve for the normal-mode frequencies and shapes of the continuous beam, after which we will find them for the cellular beam. If we assume that $y(x,t)$ can be written

$$y(x,t) = X(x)T(t) \qquad (1\text{-}19)$$

as in Section 1.2, we find that the time-dependent solution T(t) is the sinusoidal oscillation of frequency β given by Equation (1-22), and that X(x) satisfies the equation

$$\frac{d^4X(x)}{dx^4} - \beta^2 X(x) = 0 \qquad (4\text{-}3)$$

The general solution to this equation includes both circular and hyperbolic functions. Thus

$$X(x) = C_1\cos\sqrt{\beta}x + C_2\sin\sqrt{\beta}x + C_3\cosh\sqrt{\beta}x + C_4\sinh\sqrt{\beta}x \qquad (4\text{-}4)$$

However, the boundary conditions given in Equation (4-2) require that

$$X(0) = \frac{d^2X(0)}{dx^2} = X(1) = \frac{d^2X(1)}{dx^2} = 0 \qquad (4\text{-}5)$$

For these conditions to be met only the $\sin\sqrt{\beta}x$ solution above is appropriate, and

$$X(x) = C_2\sin\sqrt{\beta_n}\,x = C_2\sin n\pi x, \quad n = 1, 2, 3, \ldots \qquad (4\text{-}6)$$

Note that the boundary conditions at both ends can be met only for the discrete values β_n of the frequency parameter β, as indicated. Thus

$$\beta_n = n^2\pi^2, \quad n = 1, 2, 3, \ldots \qquad (4\text{-}7)$$

are the normal-mode frequencies in terms of the dimensionless time variable t. For the actual frequencies ω_n of a uniform hinged-hinged beam we have from Equation (1-13)

$$\omega_n = \frac{1}{L^2}\sqrt{\frac{EI}{\rho}}\,\beta_n = n^2\pi^2\sqrt{\frac{EI}{\rho L^4}} \qquad (4\text{-}8)$$

Evidently the mode shapes are sinusoidal.

Let us now proceed to solve for the normal-mode frequencies and slopes when the difference method is used. According to Equation (2-10) and (2-11) the equation of motion for the i-th cell of an unforced uniform hinged-hinged beam is given by

$$\frac{d^2y_i}{d\tau^2} + y_{i+2} - 4y_{i+1} + 6y_i - 4y_{i-1} + y_{i-2} = 0 \qquad (4\text{-}9)$$

Since we are looking for the normal modes, we assume that y_i varies as $\sin \lambda_n \tau$, where λ_n is the frequency of the n-th mode. Let us also assume that the normal-mode shapes for the cellular hinged-hinged beam are the same as those for the continuous beam, i.e., sinusoidal. Then for the n-th mode

$$y_i = a \sin \frac{n\pi i}{N} \sin \lambda_n \tau \qquad (4\text{-}10)$$

Here we are considering an N cell beam, and since $\Delta X = 1$, the beam length is N. It is evident that Equation (4-10) satisfies the boundary conditions $y_o = M_o = 0$ and $y_N = M_n = 0$. Substituting Equation (4-10) into (4-9) we find that

$$\lambda_n^2 = 2(3 - 4\cos \frac{n\pi}{N} + \cos \frac{2n\pi}{N}) \qquad (4\text{-}11)$$

is the expression for the normal-mode frequency λ_n. After expanding the cosine functions in Equation (4-11) in a power series, it follows that

$$\lambda_n = (\frac{n\pi}{N})^2 \left[1 - \frac{1}{6} (\frac{n\pi}{N})^2 + \ldots \right]^{1/2} \qquad (4\text{-}12)$$

This gives the normal-mode frequencies λ_n of the cellular hinged-hinged beam in terms of the time variable τ. From Equations (1-13) and (2-5) the actual frequency is $(N^2/L^2)\sqrt{EI/\rho}$ times λ_n. Remembering this we see that the frequency given by Equation (4-12) reduces to that for the continuous beam given in Equation (4-8) when the number of cells N becomes infinite.

For finite N the frequency λ_n is somewhat lower than the equivalent frequency for the continuous beam. A plot of the percentage deviation in normal-mode frequency versus the number of cells is shown in Figure 4-1 for the first five modes.

4.2 Uniform Cantilever Beam

Let us next solve for the normal-mode frequencies and shapes of a

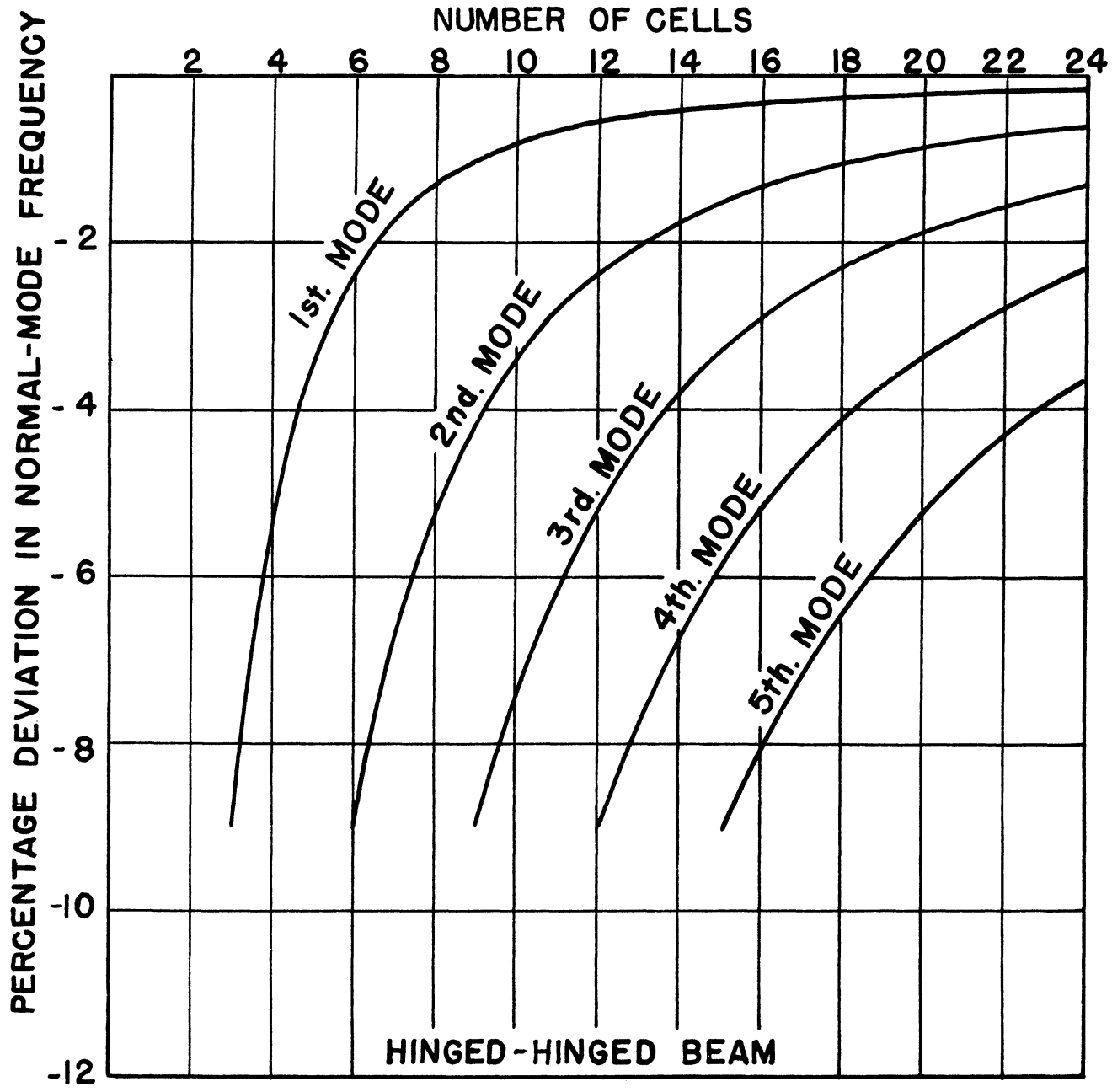

Figure 4-1

Normal-Mode Frequency Deviation for a Uniform Hinged-Hinged Beam

uniform cantilever beam. Here the fundamental equation for the continuous beam is still Equation (4-1), but the boundary conditions are

$$y(0,t) = \frac{\partial y(0,t)}{\partial x} = \frac{\partial^2 y(1,t)}{\partial x^2} = \frac{\partial^3 y(1,t)}{\partial x^3} = 0 \qquad (4\text{-}13)$$

After separation of variables Equation (4-3) is again obtained as the equation describing X(x). Equation (4-4) is the general solution, and the boundary conditions are used to eliminate the arbitrary constants. The resulting equation for β, the normal-mode frequency, is transcendental and is given by[8]

$$\cos\sqrt{\beta}\,\cosh\sqrt{\beta} = -1 \qquad (4\text{-}14)$$

The values of β_n for the first six modes, as obtained from Equation (4-14), are as follows:

Normal-Mode Frequency Parameters
for a Continuous Uniform Cantilever Beam

Mode	1	2	3	4	5	6
β_n	3.516	22.03	61.70	120.91	199.8	298.6

The task of finding the normal-mode frequencies λ_n for the uniform cellular cantilever beam does not turn out to be as simple as for the hinged-hinged beam. Instead the set of simultaneous ordinary differential equations must be solved for λ_n for each number of cells N under consideration. We have been unable to derive a general formula similar to Equation (4-11). In Figure 4-2 the percentage deviation in normal-mode frequency versus the number of cells is plotted for the first five modes for up to 16 cells. The curves were obtained by comparing the λ_n frequencies for the cellular cantilever beam with the values of β_n given in the table following Equation (4-14).

The normal-mode shapes can also be calculated for the cellular beam once the frequencies are known (see Appendix II). In Figure 4-3 the theoretical cellular-mode shapes are compared with the continuous ones for 4 and 8-cell beams. Note that when only 4 cells requiring 9 operational amplifiers are used, the mode shapes agree fairly well through the third mode, which is the maximum mode a 4-cell beam can have.

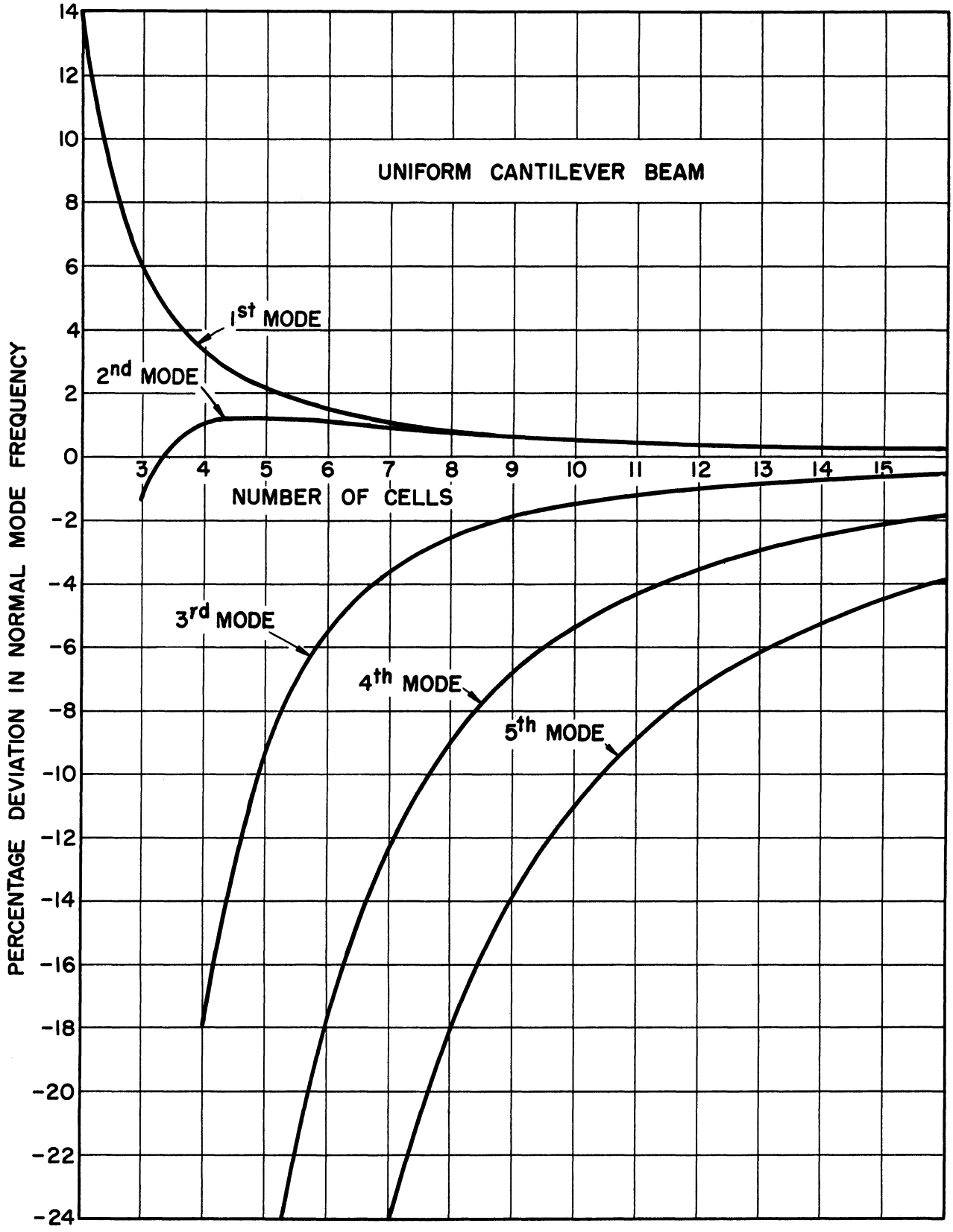

Figure 4-2 Normal-Mode Frequency Deviation for a Uniform Cantilever Beam

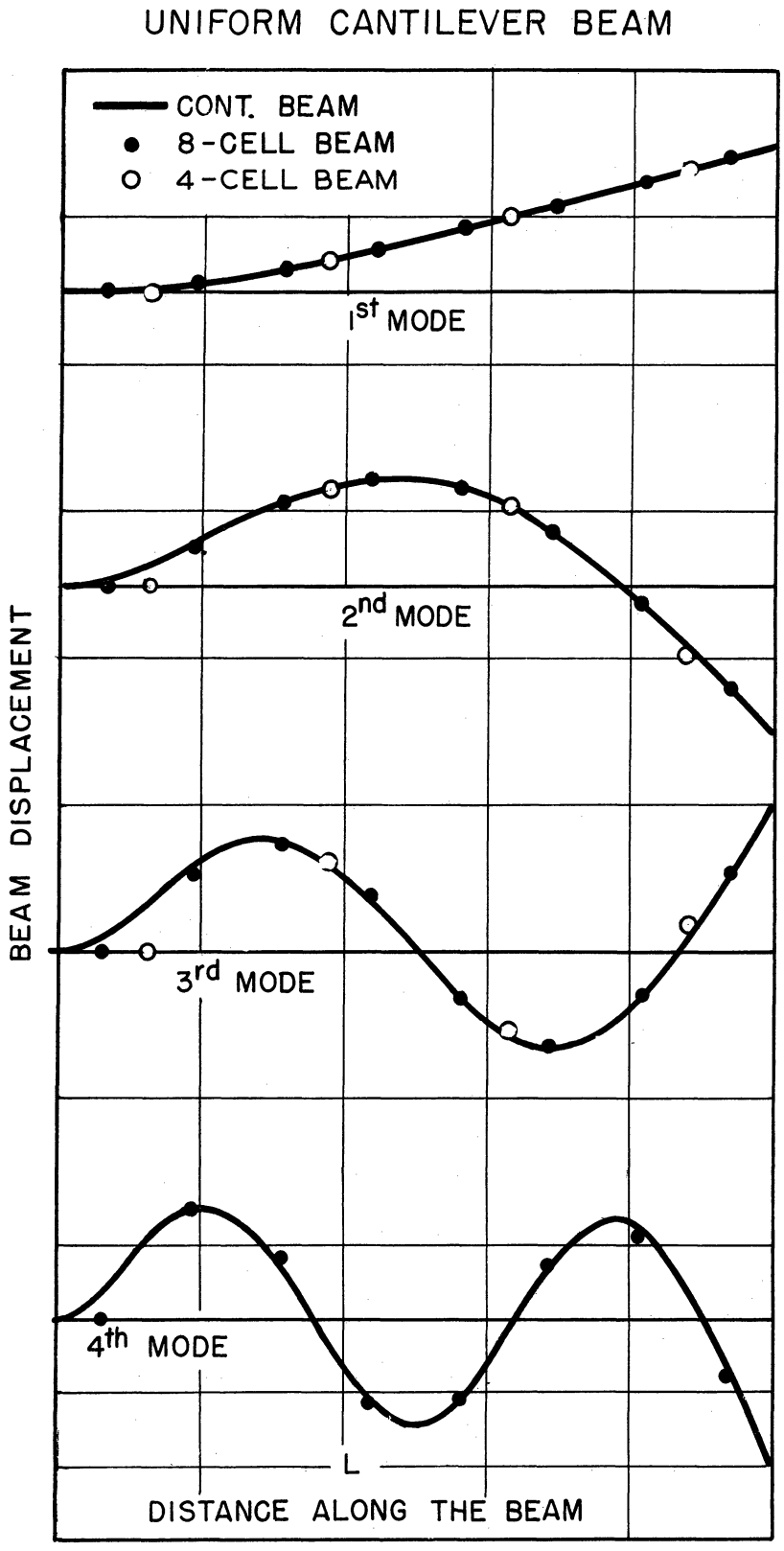

Figure 4-3

Comparison of Mode Shapes for Cellular and Continuous Uniform Cantilever Beams

4.3 Uniform Free-Free Beam

Finally we will consider a free-free or completely unsupported beam. Here the boundary conditions are

$$\frac{\partial^2 y(0,t)}{\partial x^2} = \frac{\partial^3 y(0,t)}{\partial x^3} = \frac{\partial^2 y(1,t)}{\partial x^2} = \frac{\partial^3 y(1,t)}{\partial x^3} = 0 \qquad (4\text{-}15)$$

The procedure for finding the normal-mode frequencies and shapes for the continuous beam is the same as that outlined in the previous sections. The frequency equation is [8]

$$\cos\sqrt{\beta}\,\cosh\sqrt{\beta} = 1 \qquad (4\text{-}16)$$

Values of β_n for the first five modes are as follows:

Table II
Normal-Modes Frequency Parameters
for a Continuous Uniform Free-Free Beam

Mode	1	2	3	4	5
β_n	22.37	61.67	120.91	199.8	298.6

As in the case of the cantilever beam, we were unable to find any general formula for the normal-mode frequencies for the cellular free-free beam. Instead the eigenvalues λ_n were calculated from the secular equation for each number of cells N, as explained in Appendix I. In Figure 4-4 we have plotted the number of cells versus the percentage deviation of normal-mode frequencies for the cellular free-free beam from the continuous beam frequencies. Note that the deviations for modes 1, 2, 3, and 4 are similar to those for modes 2, 3, 4, and 5 respectively for the cantilever beam (see Figure 4-2).

In Figure 4-5 the normal-mode shapes of the uniform cellular beam are compared with those of the continuous beam. Again agreement looks excellent.

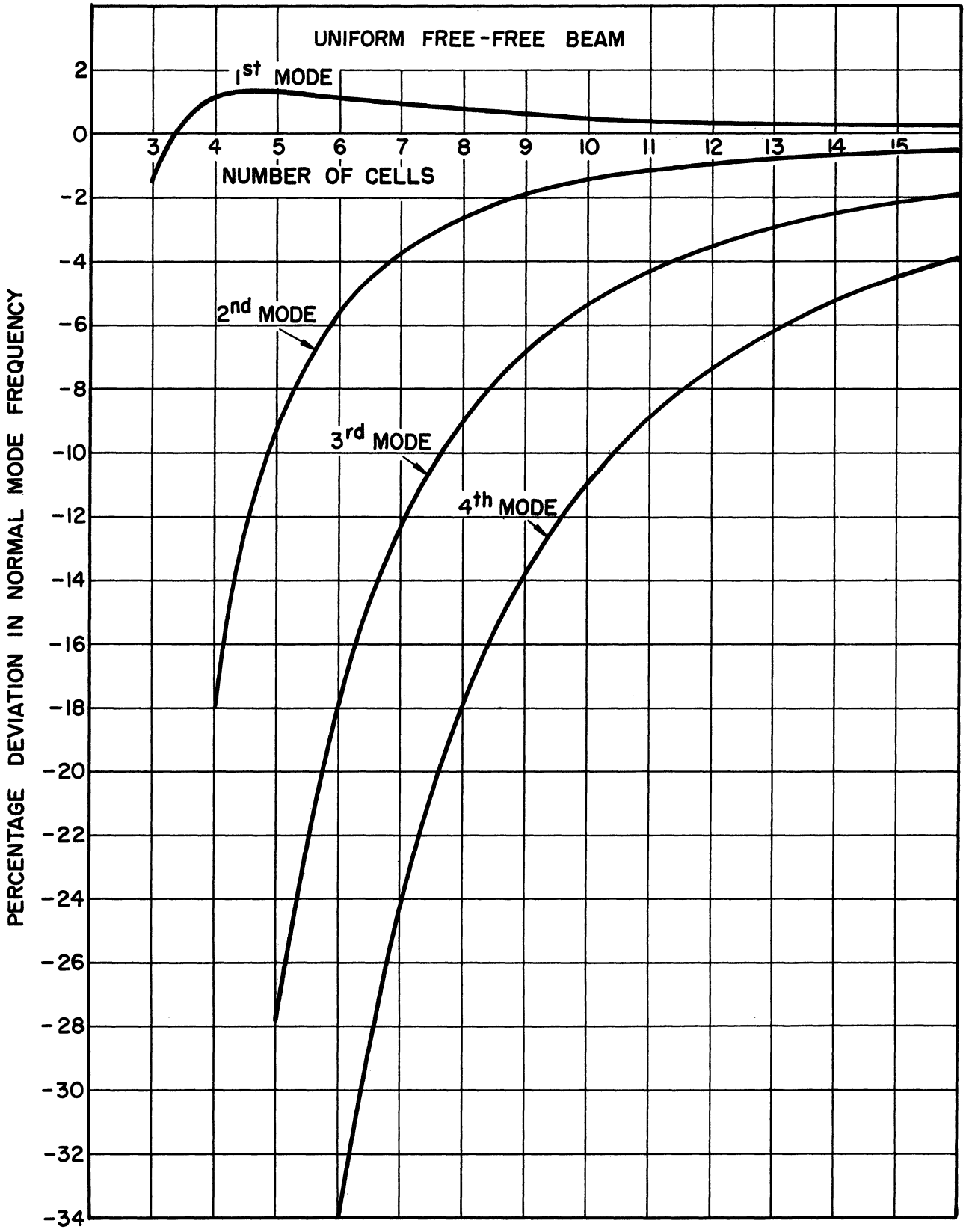

Figure 4-4

Normal-Mode Frequency Deviation for a Uniform Free-Free Beam

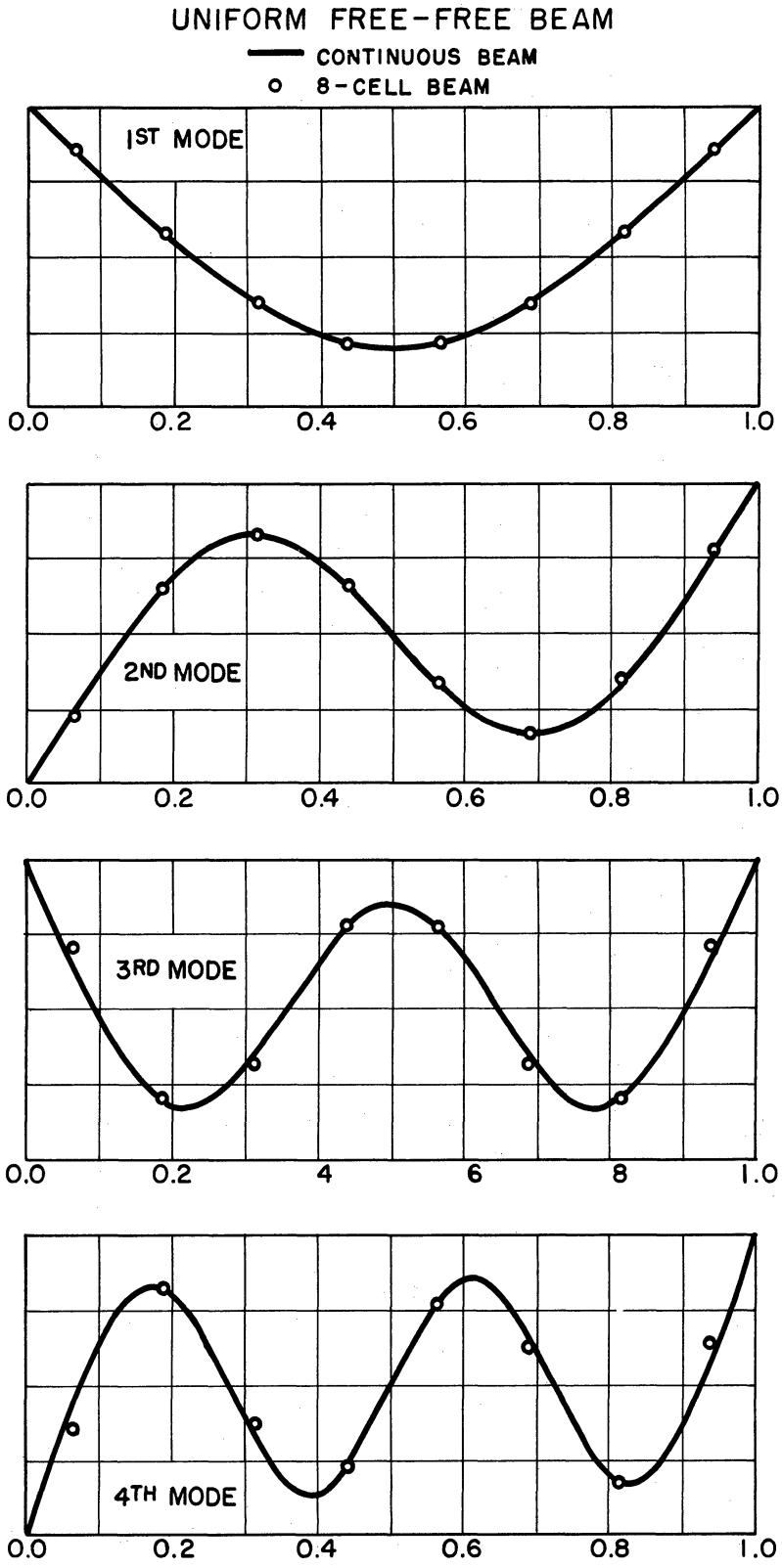

Figure 4-5

Comparison of Mode Shapes for Cellular and Continuous Free-Free Beams

4.4 Summary of Theoretical Accuracy Calculations of the Difference Techniques for Beams

We have compared theoretical normal-mode frequencies and shapes for cellular and continuous uniform hinged-hinged, cantilever, and free beams. For the hinged-hinged beam the mode shapes agree exactly; and the mode frequencies are slightly low, particularly for the higher modes or if fewer cells are used. For the cantilever and free-free beams the mode shapes agree fairly accurately, while the frequencies agree more closely than for the hinged-hinged beam. As a result of these calculations we can be confident that reasonably accurate results will be obtained for transverse vibrations of beams using the difference method when the motions are arbitrary.

CHAPTER 5

APPLICATION TO CANTILEVER BEAMS

5.1 Transient Response of a Uniform Cantilever Beam

Now that we have discussed the theoretical accuracy capabilities of the difference technique we proceed to some example solutions of transverse vibrations of beams. The electronic differential analyzer circuit for solving a cantilever beam by the difference technique was given in Figure 3-2. If the beam is uniform, $\phi_{f_n} = \phi_{d_n} = 1$. The circuit for an 8-cell uniform beam was set up on the analyzer with R = 0.2 megohms and C = 1 microfarad, giving an integrator scale factor of 0.2 seconds. Thus one unit of the dimensionless time variable τ equals 0.2 seconds in the computer solution.

In Figure 3-3, the response curves following a force impulse were shown. In Figure 5-1 the bending-moment curves following this same type of input function are shown. Note how the higher modes show up much more in the bending-moment curves.

5.2 Static Deflection for a Uniform Load

Next a uniform force was applied to all the stations. By means of resistors placed across those integrating amplifiers having velocity as their output, we were able to damp vibrations resulting from the application of the uniform force. The resulting constant beam deflection at each of the stations represents the static deflection of the beam with uniform loading. Let us compute the theoretical static deflection for a continuous beam. The equivalent equation describing the continuous beam is from Equation (2-7)

$$\frac{d^4y}{dX^4} = \Phi \quad , \text{ constant} \tag{5-1}$$

The solution to this equation with the cantilever boundary conditions (built-in end at $X = 0$, free end at $x = N$) is

$$\frac{y}{\Phi} = \frac{X^4}{24} - \frac{NX^3}{6} + \frac{N^2X^2}{4} \tag{5-2}$$

where N is the number of cells and represents the length of the beam since

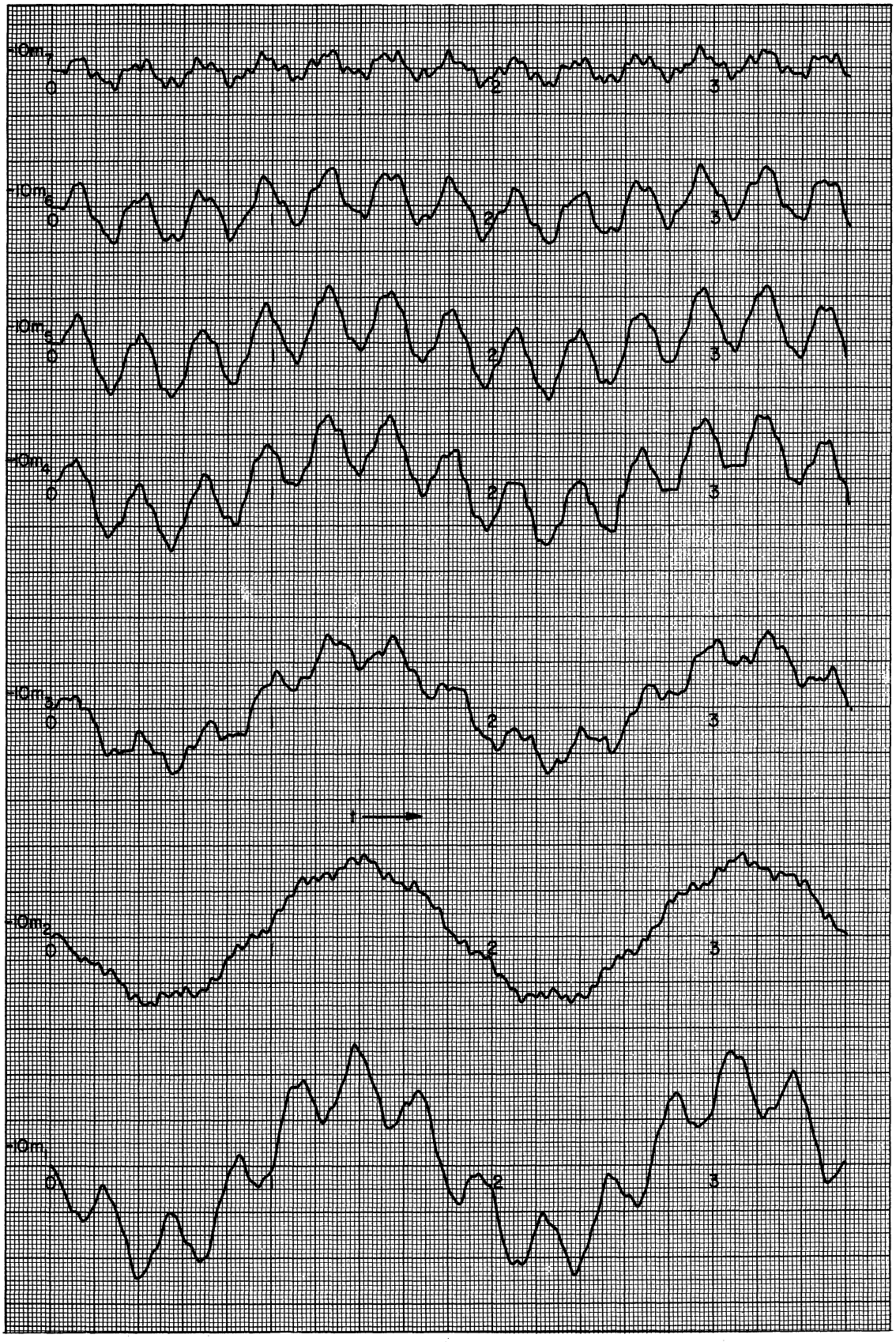

Figure 5-1

Bending-Moment Response of 8-cell Cantilever Beam to a Uniform Impulse

$\Delta x = 1$. For the problem under consideration $N = 8$. From Figure 4-3 it is clear that $X = 0.5, 1.5, 2.5$, etc., represent the values of X for y_1, y_2, y_3 etc. respectively.

In the table below the static computer deflection at each station is compared with the theoretical deflection given by Equation (5-2). Note that the displacement y_1 next to the built-in end is zero in the analyzer solution because of the built-in boundary condition for the difference method.

Table III

Comparison of Static Deflection of an 8-cell Uniform Cantilever Beam under Uniform Load with the Theoretical Deflection for a Continuous Beam

X	Station	$\frac{y}{\Phi}$ for Cont. Beam	$\frac{y}{\Phi}$ from the Analyzer
0.5	1	3.8	0.0
1.5	2	31.3	28.0
2.5	3	80.8	77.5
3.5	4	145.0	141.0
4.5	5	219.6	216.0
5.5	6	300.0	295.0
6.5	7	384.0	379.0
7.5	8	469.0	461.0

5.3 Determination of Normal Mode Frequencies

The normal mode frequency parameters for a continuous uniform cantilever beam of unit length were given in Section 4.2. The frequency parameters for a beam of length N will be just $1/N^2$ times those given in 4.2. For a cellular beam these frequencies will of course be subject to the deviations shown in Figure 4-2. Thus for our 8-cell uniform cantilever beam the frequency f_1 of the first mode will be

$$f_1 = \frac{3.516(1 + 0.008)}{2\pi (64)} = 0.00882 \text{ cycles/unit } \tau$$

Since one unit of computer time τ equals 0.2 seconds in our analyzer circuit, the expected frequency in cycles per second for the first mode is 0.00882/0.2 or 0.0441 cycles per second. This represents a period of 22.7 seconds. The calculation of expected frequencies for higher modes of the 8-cell cantilever beam follows the same procedure outlined above.

The next problem is to excite the normal modes of the actual beam circuit which is set up on the electronic differential analyzer. We found that this could be done very effectively by driving the beam at antinodal points with a sinusoidal frequency approximately equal to the normal-mode frequency. The amplitude of the sinusoidal driving voltage is started at zero and is slowly increased until the sinusoidal beam response becomes appreciable. The sinusoidal input voltage is then held constant until the response builds up to the desired amplitude, e.g. 20 to 50 volts at the antinodes. The amplitude of the sinusoidal input is then slowly decreased to zero. The computer circuit representing the beam then continuous to oscillate harmonically with constant amplitude at the excited normal-mode frequency. In Figure 5-2 the input forcing function is shown along with the response for an excitation of the second mode of our 8-cell uniform cantilever beam. The beam was driven at stations 4 and 8, and output displacements and velocities at these antinodal points were recorded.

By using the sinusoidal forcing technique described in the previous paragraph one can excite almost a pure modal oscillation with a minimum of transients. It is often necessary to readjust the forcing frequency after an approximate experimental determination of the normal-mode frequency. For modes higher than the first it is usually best to record the output velocity rather than displacement, since in the velocity outputs the relative amount of first mode which may have inadvertantly been excited is reduced in comparison with the higher modes.

In the table below are shown the percentage deviations in normal-mode frequencies for the 8-cell analyzer beam from the theoretical frequencies for a continuous cantilever beam. In addition, the theoretical deviations for the 8-cell beam are shown. Evidently the computer deviations agree closely with the theoretical deviations. Computer components were calibrated to within several hundredths of a per cent for these tests.

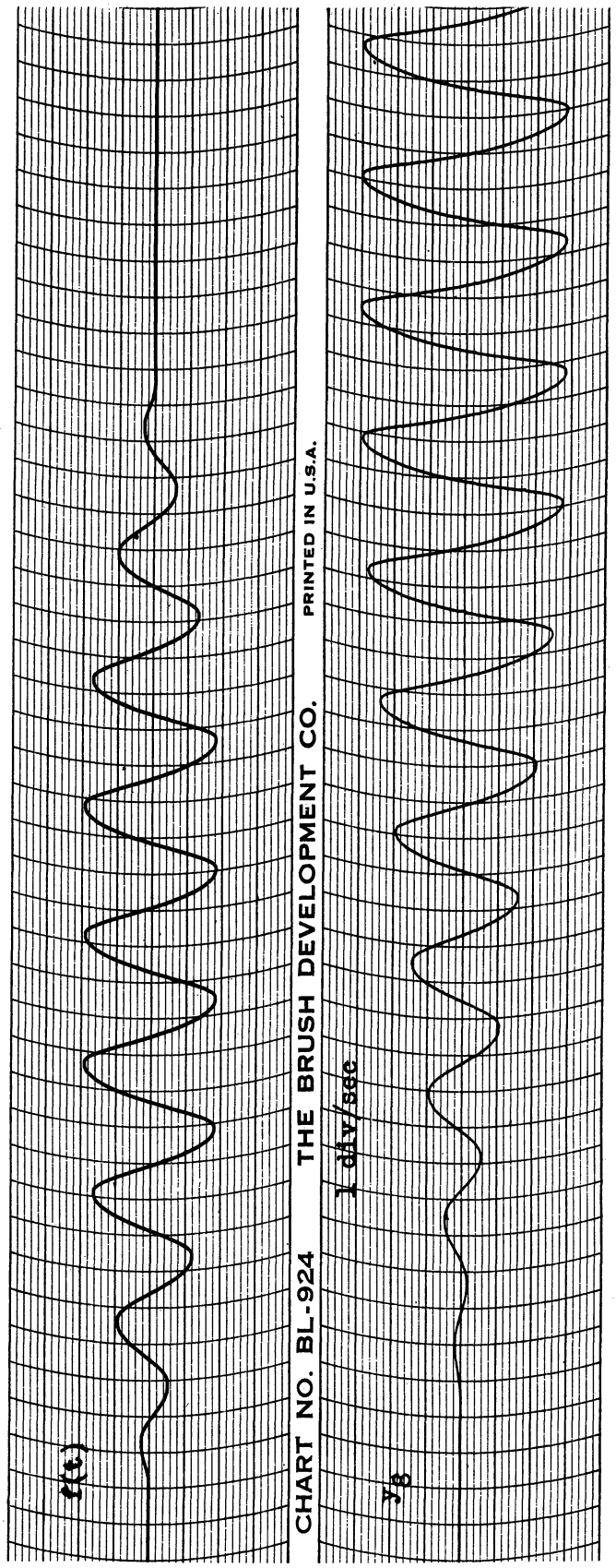

Figure 5-2 Excitation of the Second-Mode of an 8-cell Cantilever Beam

Table IV

Normal Mode Frequency for a Uniform Cantilever Beam

Beam Length = N = 8

Mode	Continuous Beam	Deviation for 8-Cell Computer	Deviation for 8-Cell Theoretical
1	0.0437	0.94%	0.72
2	0.275	-0.51	-0.72
3	0.768	-2.48	-2.56
4	1.507	-8.85	-8.67

5.4 Component Accuracy Requirements

One of the fundamental difficulties encountered when continuous derivatives are replaced by finite differences involves accuracy requirements; the smaller the interval between stations, the higher the accuracy required in taking the difference. In the case of the vibrating beam, it is evident that the greater the number of cells for any half-wave length of a normal mode, the smaller the differences which represent second derivatives become and the more critical the accuracy requirements become for the summing resistors.

For example, in the first mode of oscillation of a uniform 8-cell cantilever beam the differences representing bending-moments and accelerations are quite small compared with the displacements. If the circuit shown in Figure 3-2, it turns out that a one percent error in only one of the 36 summing resistors will change the frequency the fundamental mode by about one percent. The departure from the correct frequencies for the higher modes will be less seriously effected.

The uniform beam can be solved by computing $\partial^4 y/\partial x^4$ at the n-th station directly, so that the equation at the n-th cell is

$$\frac{d^2 y}{d\tau^2} = -y_{n+2} + 4y_{n+1} - 6y_n + 4y_{n-1} - y_{n-2} \qquad (5\text{-}3)$$

If the differential analyzer is connected to solve the problem in this manner, i.e., by computing the fourth derivative as a fifth-order difference, the accuracy of summing resistors becomes even more critical. A one-per cent

error in one of the summing resistors for only a 5-cell cantilever beam perturbs the fundamental frequency by about 5 per cent.[6] For 8 cells or higher the summing-resistor accuracy requirements are even more critical.

It is felt that for cantilever beams up to 10 cells, 0.1 per cent accuracy is adequate for summing resistors when about 1 per cent over-all accuracy is desired.

5.5 Effect of Voltage Transients

The deflection of a beam due to an applied force is proportional to the fourth power of the length of the beam. This is apparent in Equation (5-2), where the length of the cantilever beam is N, and where the deflection y(N) at the free end is given by $(3\Phi/24)N^4$. The deflections along the beam are represented on the electronic differential analyzer by voltage outputs of amplifiers. These latter voltages may be deliberately introduced through appropriate input resistors or may be inadvertantly introduced through steady unbalances in summing amplifiers or transient shifts in amplifier balances. As a result, beam oscillations may be excited by fluctuations in the power supply voltages. The sensitivity of the network to such small voltage inputs will increase as the fourth power of the number of cells.

Thus it becomes important to have well-regulated power supplies which are free from any sudden fluctuations.[2] Drift-stabilized amplifiers serve to reduce the long-term amplifier drifts.[2, 10, 12, 13] In order to test the magnitude of unwanted transient oscillations which can occur, 5 and 8-cell uniform cantilever beams were set up on the electronic differential analyzer using drift-stabilized amplifiers. Zero initial displacements and velocities were used, and beam displacements were recorded after the release of the initial conditions. As a result of initial unbalances in the amplifiers transient first-mode oscillations of 6 and 40 millivolts amplitude were recorded for the 5 and 8-cell beams, respectively. The disproportionately larger amplitude for the 8-cell beam was probably the result of small unbalances due to circulating ground currents between relay racks (one rack was required for the 5-cell beam, two racks for the 8-cell beam). After release of the initial conditions the first-mode oscillation grew about

1 millivolt per first-mode cycle as a result of transient voltage inputs (presumably from the power supplies). Since ±100 volts is the full-scale computer output, none of the above effects are considered serious.

5.6 Tapered Cantilever Beam

In order to evaluate the accuracy of the difference method for non-uniform beams, the tapered cantilever beam shown in Figure 5-3 was set up on the electronic differential analyzer. The beam had a taper-ratio of 2:1 in both chord and thickness and could represent an aircraft wing. Use of the built-in boundary condition implies that the wing mass is small compared with the mass of the fuselage. Two problems were solved: (1) the tapered beam alone, and (2) the tapered beam with the addition of a concentrated mass load at station 8. This load simulates a wing tank of half the mass of the wing.

A gust load of one-second duration was applied as a force proportional to the chord at each cell. Figure 5-4 is a recording of the displacement at station 8 and also shows the gust load. An integrator time scale of 0.2 seconds was used in this solution.

The normal-mode frequencies were obtained for the 8-cell beam with and without the wing tank. These are tabulated below along with the values for the normal-mode frequencies obtained by a differential-analyzer solution of the continuous problem.

Table V

Normal-Mode Frequencies of the Tapered Beam

Mode	Continuous Beam (No Wing Tank)	8-Cell Beam (No Wing Tank)	8-Cell Beam (Wing Tank)
1	0.00773 cps	0.0767 cps	0.0372
2	0.331	0.326	0.256
3	0.820	0.784	0.709
4		2.016	2.000

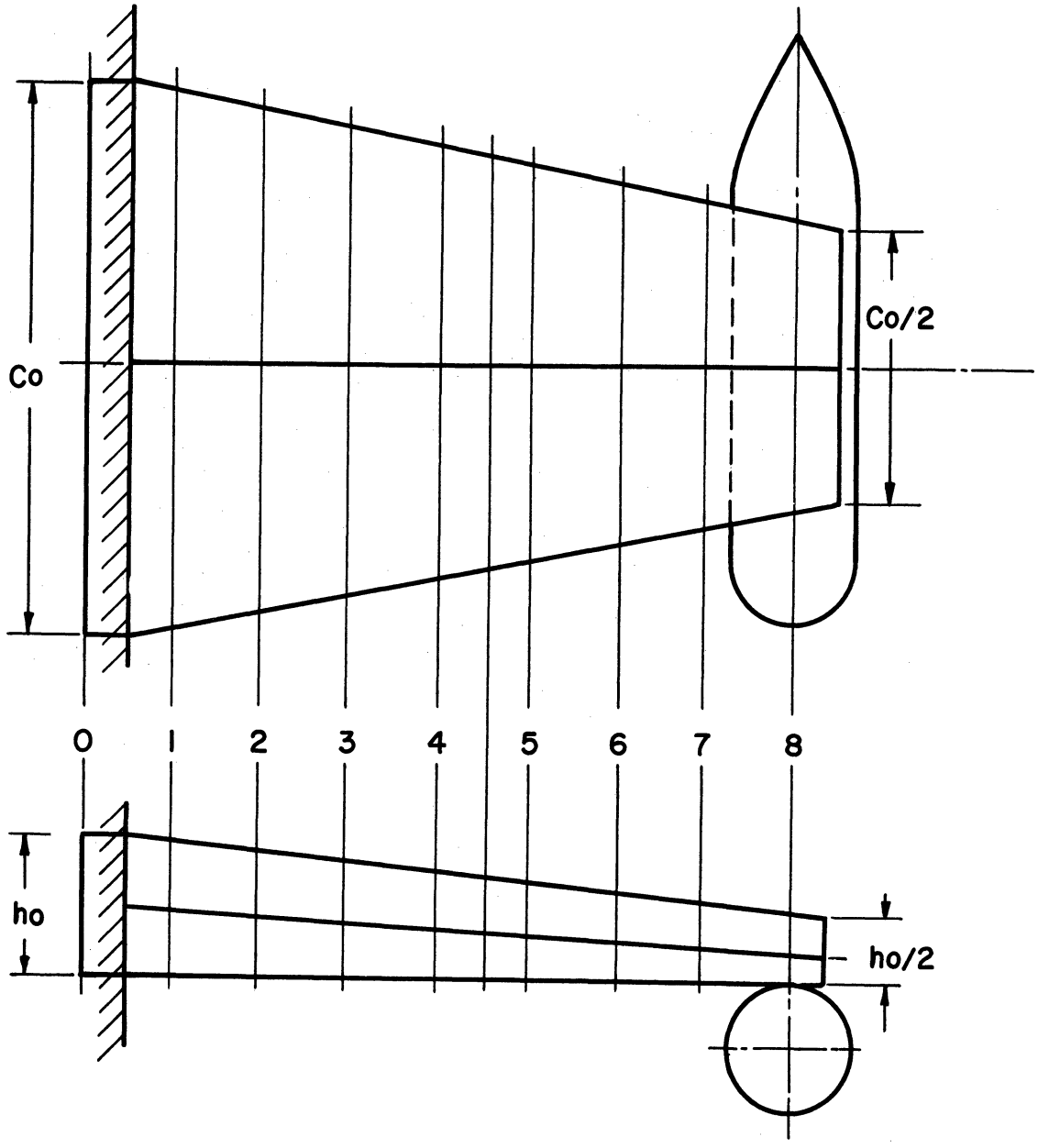

Figure 5-3
Tapered Cantilever Beam with Concentrated Mass Load

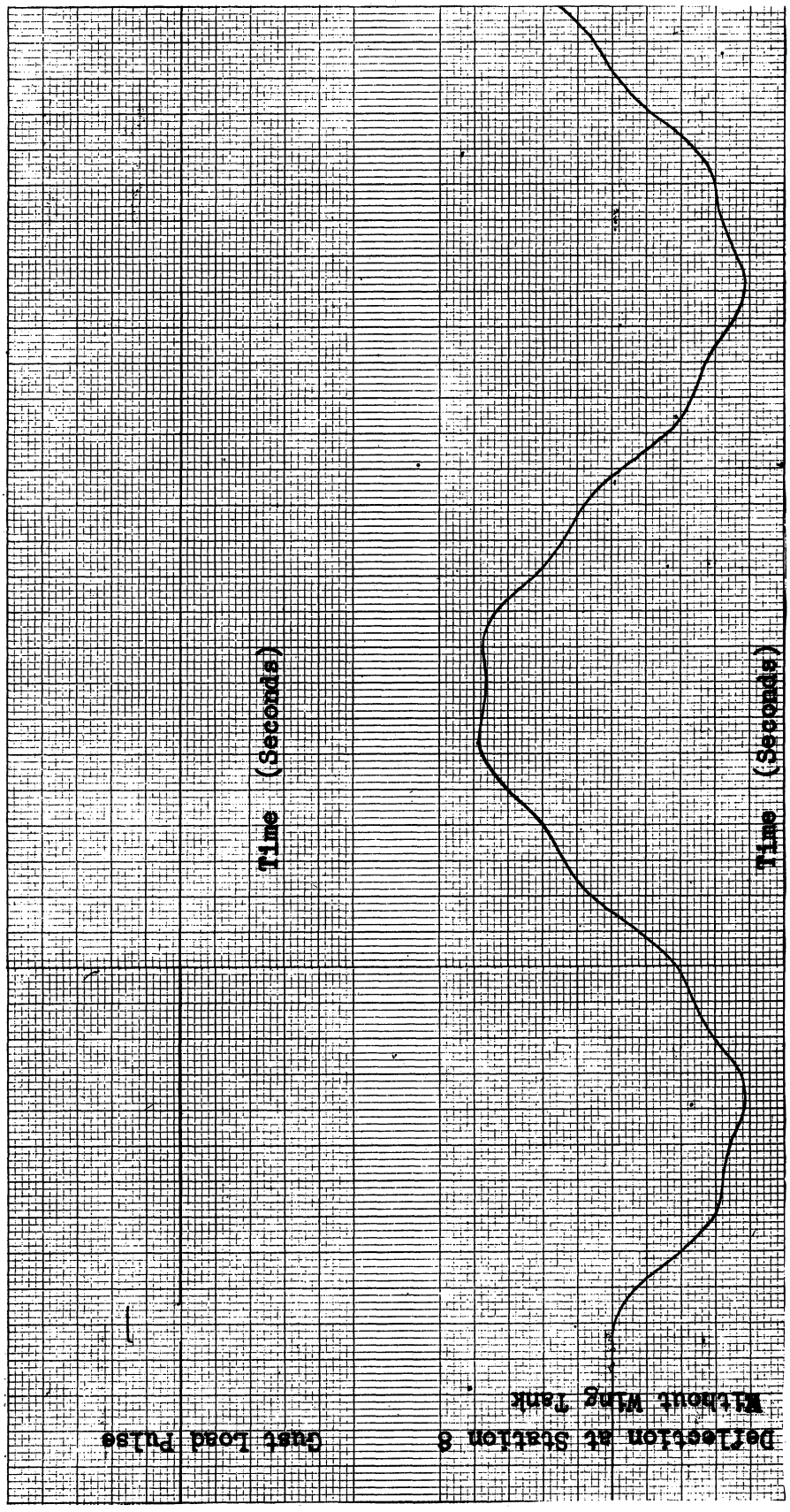

Figure 5-4 Displacement at Wing-Tip Following a One-Second Uniform Impulse

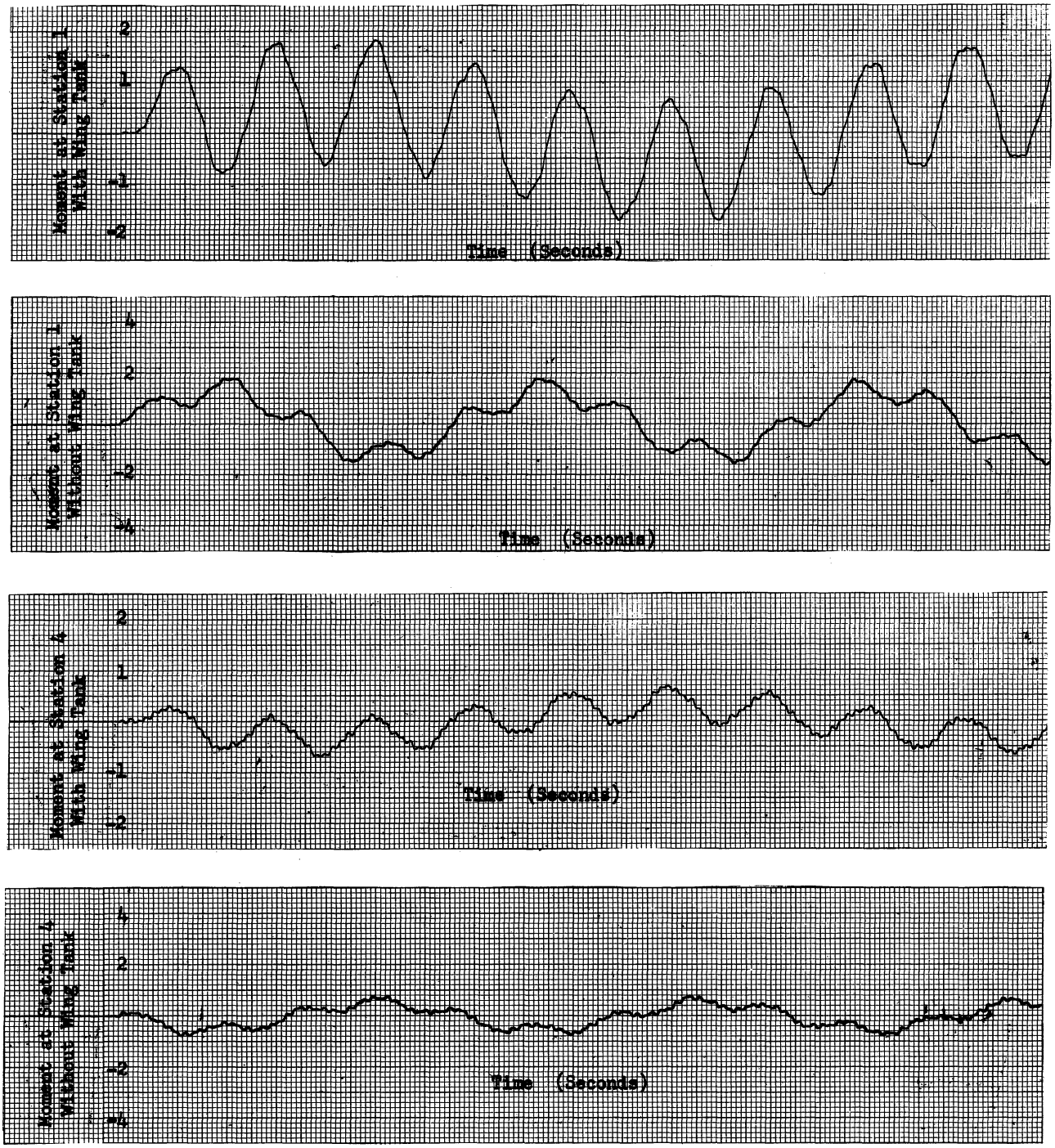

Figure 5-5

Comparison of the Moments at Stations 1 and 4 of the Tapered Cantilever Beam with and without the Concentrated Mass Load

In Figure 5-5 the moments near the root (station 1) and near mid-span (station 4) are recorded for the cases with and without the wing tank. For both recordings identical one-second gust loads were applied.

5.7 Uniform Cantilever Beam with Concentrated Mass Load at the Free End

In the previous section we solved a tapered cantilever beam with a concentrated load at the free end. Actually, the concentrated mass occurs 1/2 station from the free end, as is evident in Figure 5-5 and also in Figure 5-6 below. If the beam under consideration has the concentrated mass located at the true end (station 8 1/2 in Figure 5-6), then an error will result in the

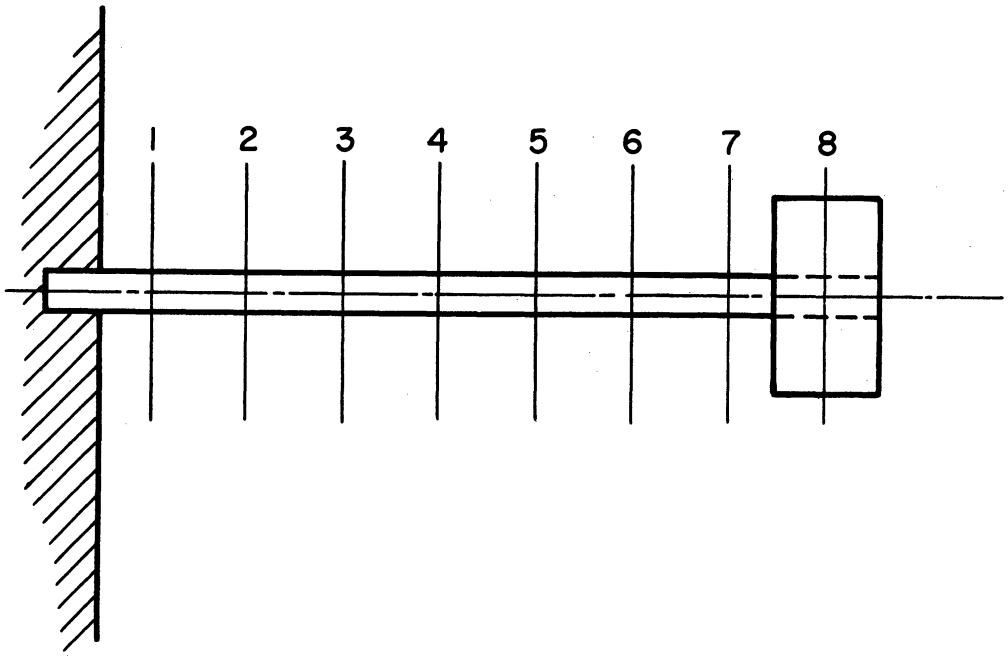

Figure 5-6
Uniform Cantilever Beam with Concentrated Mass Load at the Free End

difference approximation. The larger the concentrated mass M_L, the bigger will this error be. In order to investigate this effect, the uniform 8-cell contilever beam shown in Figure (5-6) was considered. Let us denote the

concentrated mass at station 8 as M_L, and the total mass of the uniform beam by M_B. Normal-mode frequencies of the 8-cell beam for various M_L/M_B ratios will be compared with theoretical frequencies when M_L occurs at the exact end of a continuous beam. In this way we can estimate the error which results from locating the mass at a point 1/2 station from the end.

Manley[9] gives the following equation for the first-mode frequency of a cantilever beam with a concentrated mass load at the free end

$$\omega^2 = \frac{3.04\ EI}{\rho L^4} \quad \frac{1}{\frac{M_L}{M_B} + 0.226} \tag{5-4}$$

If we let

$$\beta_L^2 = \frac{3.04}{\frac{M_L}{M_B} + 0.226} \tag{5-5}$$

then

$$\omega = \frac{1}{L^4}\sqrt{\frac{EI}{\rho}}\,\beta_L \tag{5-6}$$

which is similar to Equation (4-8). Thus β_L represents the dimensionless frequency parameter for the first mode and will be different for each ratio of M_L/M_B.

Timoshenko[8] derives a slightly different relation for the frequency of the end-loaded cantilever beam. His formula is

$$\beta_L^2 = \frac{3}{\frac{M_L}{M_B} + \frac{33}{140}} \tag{5-7}$$

Both Equations (5-5) and (5-7) predict a linear variation of $1/\beta_L^2$ with M_L/M_B

The electronic differential analyzer was used to find the first-mode frequencies and hence β_L for an 8-cell cantilever beam. An integrator scale factor of 0.2 seconds was employed with R = 0.2 megohms and C = 1 microfarad. Also, $\phi_{f_1} = 1$, $\phi_{f_2} = 1$, ... $\phi_{f_8} = 1$, and $\phi_{d_1} = 1$, $\phi_{d_2} = 1$, ... $\phi_{d_7} = 1$, $\phi_{d_8} = 1 + 8M_L/M_B$. The normal modes were excited by sinusoidal forcing voltages as described in Section 5.3. The computer frequencies were multiplied by RCN^2 (= 0.2(64) = 12.8) in order to obtain β_L. In the table below the first mode frequencies are compared with those given by Equation (5-5) for various M_L/M_B. From the table it is

Table VI

First-Mode Frequencies for Uniform Cantilever Beam with Concentrated Mass at the Free-End

M_L/M_B	β_L (8-cell computer)	Percentage Deviation from Equation (5-5)
0	3.549	-2.7%
1/8	2.973	0.0
1/4	2.602	2.9
1/2	2.154	5.1
1	1.683	6.3
2	1.264	7.5
4	0.9229	8.9
6	0.7630	9.1
8	0.6630	9.1

evident that for $M_L/M_B < 1/2$ the error in the 8-cell beam resulting from the mass occurring 1/2 station from the free end is fairly small. For large M_L/M_B the effective beam length becomes 7-1/2 and not 8, which accounts for the larger deviation in this region. It should be remembered that Equation (5-5) is approximate; the percentage deviations given in the table are therefore somewhat in error.

From the first-mode frequencies for the 8-cell beam the plot of $1/\beta_L^2$ versus M_L/M_B shown in Figure 5-7 was made. The following formula was obtained from the intercept and slope of the curve:

$$\beta_L^2 = \frac{3.643}{\frac{M_L}{M_B} + 0.2892} \tag{5-8}$$

The second and third-mode frequencies were also determined as a function of M_L/M_B for the 8-cell cantilever beam. The data is summarized in the table below.

Table VII

M_L/M_B	β_L Second Mode (8-cell Beam)	β_L Third Mode (8-cell Beam)
0	22.14	60.17
1/8	20.39	57.54
1/4	19.56	56.52
1/2	18.78	55.71
1	18.23	55.09
2	17.86	54.71
4	17.65	54.53
6	17.59	54.46
8	17.55	54.40

Note that β_L for the second and third modes approaches a limiting value for large M_L/M_B. For infinite M_L/M_B there can be no displacement at station 8, so that $y_8 = 0$. Since in this case the bending moment at station 8 is also zero, we have effectively a hinged end fastening. Consequently the limiting values of β_L are those for the second and third modes respectively of a built-in, hinged beam.

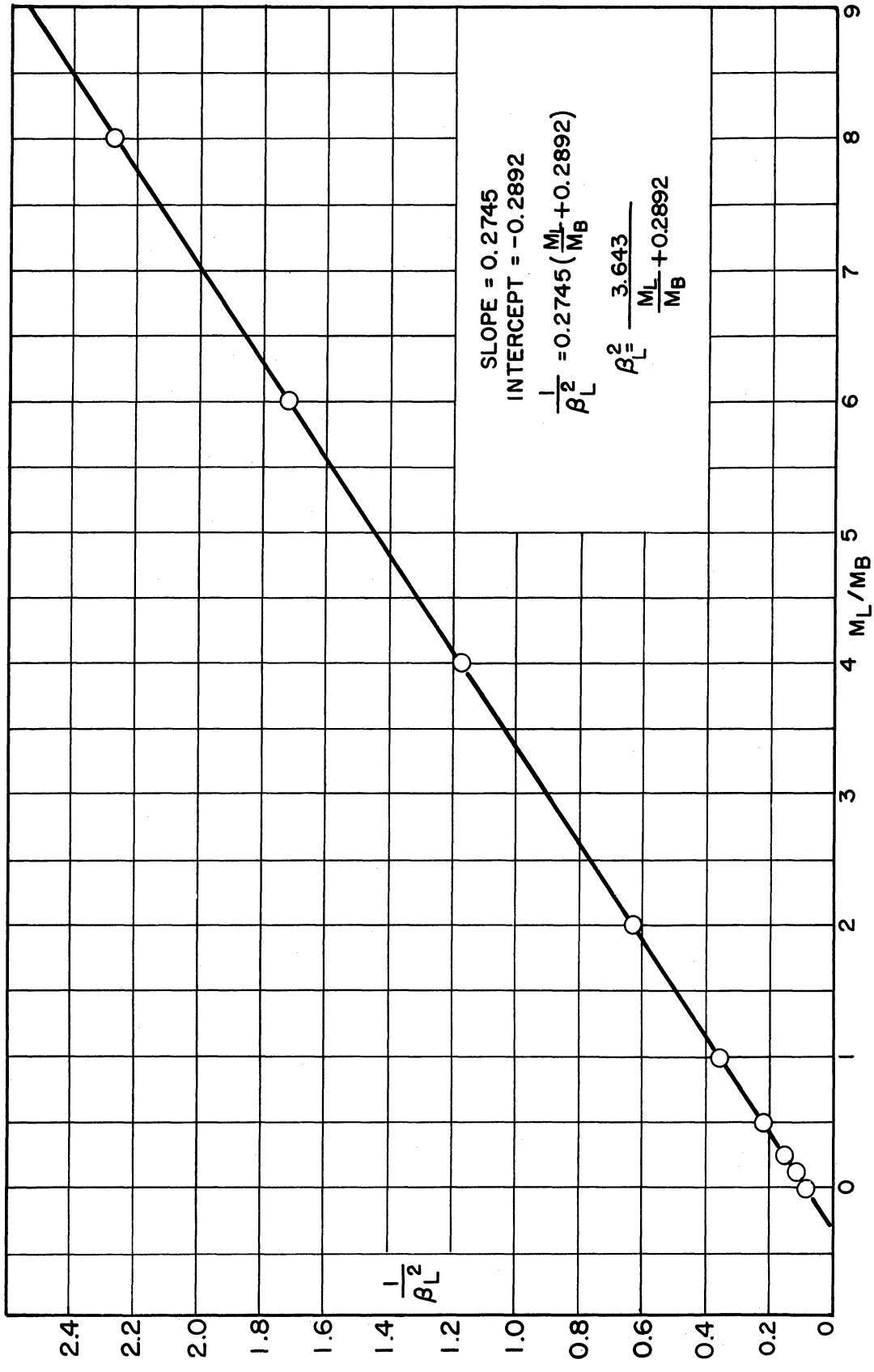

Figure 5-7 $1/\beta_L^2$ versus M_L/M_B for an 8-cell End-Loaded Cantilever Beam

CHAPTER 6

APPLICATION TO HINGED-HINGED BEAMS

6.1 Analyzer Circuit for the Hinged-Hinged Beam

In this chapter we will discuss briefly the solution of hinged-hinged beams using the difference method, first for a uniform hinged-hinged beam and then for a uniform beam with a concentrated mass at the center. Equations (2-10) and (2-11) give the equillibrium equation at the nth cell. The hinged boundary conditions are given in Table I, Section 2.2. If the ends of an N-cell hinged-hinged beam occur at $\chi = 0$ and $\chi = N$, the boundary conditions require that

$$y_o = M_o = 0$$

$$y_N = M_N = 0 \qquad (6\text{-}1)$$

From Equations (2-10), (2-11), and (6-1), the system of N - 1 equations for the N-cell hinged-hinged beam is

$$\phi_{d_1} \frac{d^2y_1}{d\tau^2} = -m_2 + 2m_1 + \Phi_1(\tau)$$

$$\phi_{d_2} \frac{d^2y_2}{d\tau^2} = -m_3 + 2m_2 - m_1 + \Phi_2(\tau)$$

$$\phi_{d_3} \frac{d^2y_3}{d\tau^2} = -m_4 + 2m_3 - m_2 + \Phi_3(\tau) \qquad (6\text{-}2)$$

$$\vdots \qquad\qquad \vdots$$

$$\phi_{d_{N-2}} \frac{d^2y_{N-2}}{d\tau^2} = -m_{N-1} + 2m_{N-2} - m_{N-3} + \Phi_{N-2}(\tau)$$

$$\phi_{d_{N-1}} \frac{d^2 y_{N-1}}{d\tau^2} = 2m_{N-1} - m_{N-2} + \Phi_{N-1}(\tau)$$

where

$$\begin{aligned}
m_1 &= \phi_{f_1}(y_2 - 2y_1) \\
m_2 &= \phi_{f_2}(y_3 - 2y_2 + y_1) \\
m_3 &= \phi_{f_3}(y_4 - 2y_3 + y_2) \qquad (6\text{-}3) \\
&\vdots \qquad\qquad \vdots \\
m_{N-2} &= \phi_{f_{N-2}}(y_{N-1} - 2y_{N-2} + y_{N-3}) \\
m_{N-1} &= \phi_{f_{N-1}}(-2y_{N-1} + y_{N-2})
\end{aligned}$$

The electronic differential analyzer circuit for solving the hinged-hinged beam by the difference method is shown in Figure (3-5). Evidently 3(N-1) amplifiers are required for an N-cell beam.

6.2 Uniform Hinged-Hinged Beam

An 8-cell uniform hinged-hinged beam was set up using the circuit of Figure 3-5. An integrator time scale of 0.2 seconds was employed. The frequencies for the first three modes were determined using techniques similar to those discussed in Section 5.3. In the table below these frequencies are compared with the theoretical frequencies obtained from Equation (4-6) for the continuous hinged-hinged beam and from Equation (4-12) for the 8-cell beam.

TABLE VIII

Normal Mode Frequencies for a Hinged-Hinged Beam

Beam Length = N = 8

Mode	Continuous Beam	Deviation for 8-Cell Computer	Deviation for 8-Cell Theoretical
1	0.1227 cps	-1.45%	-1.29%
2	0.4909	-5.00	-5.22
3	1.1045	-10.8	-11.0

6.3 Uniform Hinged-Hinged Beam with Concentrated Mass at the Center

Next we consider an 8-cell uniform beam with an additional mass at the center, as shown in Figure 6-1. The theoretical frequency of vibration for the first mode is given by[9]

$$\omega_1 = \frac{\pi^2}{L^2}\sqrt{\frac{EI}{\rho}}\;\frac{1}{\sqrt{1 + 2\,\frac{M_L}{M_B}}} \qquad (6\text{-}4)$$

where M_B is the mass of the beam and M_L is the additional mass concentrated at the center. This equation was derived by Rayleigh's method for heavy beams. For $M_L = 0$, Equation (6-4) reduces to the first-mode frequency given in Equation (4-8) for a uniform hinged-hinged beam.

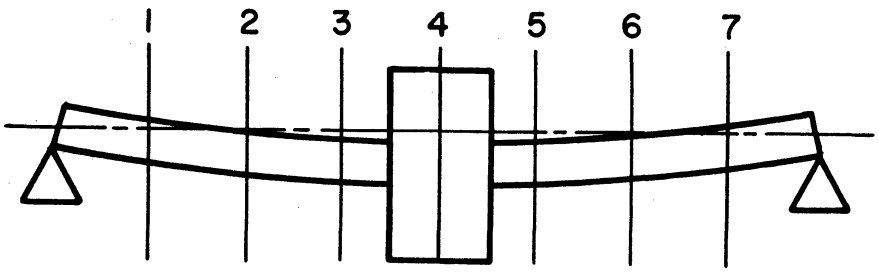

Figure 6-1

Uniform Hinged-Hinged Beam with Concentrated Mass Load at the Center

A uniform 8-cell hinged-hinged beam was set up on the differential analyzer using an integrator time scale of 0.2 seconds as before. The input resistor to the $dy_4/d\tau$ integrating amplifier was set equal to $0.2(1 + 8M_L/M_B)$ to represent the added mass M_L at the center. First-mode frequencies were determined for M_L/M_B = 1/8, 1/4, 1/2, 1, 2, 4, and 8. In addition, the second-mode frequency for M_L/M_B = 8 and the third-mode frequencies for M_L/M_B = 1/2 and 8 were found. In each case, the normal modes were excited in the manner described in Section 5.3, i.e., by driving the beam sinusoidally at antinodal points and observing the frequency after removal of the driving function.

The results are shown in Table IX below. Of particular interest is the data on the last line, which shows the second-mode frequency when M_L/M_B = 8. The frequency checks within 0.05 per cent with that obtained for M_L/M_B = 0. The two frequencies should, of course, agree since for the second mode the displacement at the center of the beam is zero, thus making the motion independent of the mass at the center.

Table IX

Uniform Hinged-Hinged Beam
with a Concentrated Mass at the Center

T_L = period of oscillation with concentrated mass M_L at center.

T_o = period of oscillation without M_L.

Mode	$\frac{M_L}{M_B}$	Period T_L (8-Cell Beam)	$\frac{T_L}{T_o}$ (8-Cell Beam)	$\frac{T_L}{T_o} = 1 + 2\frac{M_L}{M_B}$ (Theoretical)
1	0	8.268 sec	1	1
1	1/8	9.240	1.118	1.118
1	1/4	10.144	1.227	1.225
1	1/2	11.770	1.424	1.414
1	1	14.420	1.744	1.732
1	2	18.66	2.257	2.236
1	4	25.0	3.024	3.000

Table IX (continued)

Mode	$\frac{M_L}{M_B}$	Period T_L (8-Cell Beam)	$\frac{T_L}{T_o}$ (8-Cell Beam)	$\frac{T_L}{T_o} = 1 + 2\frac{M_L}{M_B}$ (Theoretical)
1	8	34.4	4.161	4.123
2	0	2.143		
3	0	1.015		
3	1/2	1.269	1.250	
3	8	1.462	1.440	
2	8	2.144		

CHAPTER 7

APPLICATION TO FREE-FREE BEAMS

7.1 Uniform Free-Free Beam

A cellular free-free beam is shown in Figure 7-1. The boundary conditions of zero bending moment and shear force at the ends are given in Table I, Section 2.2.

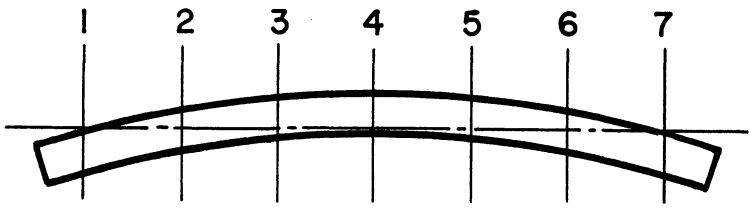

Figure 7-1
Cellular Free-Free Beam

Thus for an N-Cell free-free beam

$$M_o = M_1 = 0$$

and

$$M_N = M_{N+1} = 0 \qquad (7\text{-}1)$$

From Equations (2-10), (2-11) and (7-1) the system of N equations for the N-cell free-free beam become

$$\phi_{d_1} \frac{d^2y_1}{d\tau^2} = -m_2 + \Phi_1(\tau)$$

$$\phi_{d_2} \frac{d^2y_2}{d\tau^2} = -m_3 + 2m_2 + \Phi_2(\tau)$$

$$\phi_{d_3} \frac{d^2y_3}{d\tau^2} = -m_4 + 2m_3 - m_2 + \Phi_3(\tau)$$

$$\phi_{d_4} \frac{d^2y_4}{d\tau^2} = -m_5 + 2m_4 - m_3 + \Phi_4(\tau)$$

$$\vdots \qquad\qquad \vdots \qquad\qquad (7\text{-}2)$$

$$\phi_{d_{N-2}} \frac{d^2y_{N-2}}{d\tau^2} = -m_{N-1} + 2m_{N-2} - m_{N-3} + \Phi_{N-2}(\tau)$$

$$\phi_{d_{N-1}} \frac{d^2y_{N-1}}{d\tau^2} = 2m_{N-1} - m_{N-2} + \Phi_{N-1}(\tau)$$

$$\phi_{d_N} \frac{d^2y_N}{d\tau^2} = -m_{N-1} + \Phi_N(\tau)$$

where

$$m_2 = \phi_{f_2}(y_3 - 2y_2 + y_1)$$

$$m_3 = \phi_{f_3}(y_4 - 2y_3 + y_2) \qquad (7\text{-}3)$$

$$\vdots \qquad\qquad \vdots$$

$$m_{N-1} = \phi_{f_{N-1}}(y_N - 2y_{N-1} + y_{N-2})$$

The differential analyzer circuit is the same as that for the cantilever beam (see Figure 3-2) except that both ends have the configuration of the free end which occurs at the N+1/2 station for the cantilever beam.

Normal-mode frequencies for a 7-cell uniform cantilever beam were determined both by the sinusoidal forcing technique described in Section 5.3 and by setting initial conditions to correspond to a given mode shape. Integrator scale factors of 0.2 seconds were employed. Table X gives the observed normal-mode frequencies.

Table X

Normal-Mode Frequencies for a 7-Cell Uniform Free-Free Beam

Mode	Continuous Beam	Deviation for 7-Cell Computer	Deviation for 7-Cell Theoretical
1	0.3633 cps	0.82%	0.90%
2	1.0016	-3.70	-3.70
3	1.9638	-12.21	-12.34

7.2 Stability of the Free-Free Beam Circuit

The principal problem associated with the representation of a free-free beam arises because of the boundary conditions at the free ends, namely that those ends are not restrained in either displacement or slope. This means that the beam will exhibit steady-state translation and rotational velocities and accelerations as a result of any initial velocities or steady applied forces. Thus, any initial voltage transients or amplifier unbalances in the electronic differential analyzer will cause the computer outputs representing the beam displacements to gradually drift. In Figure 7-2 recordings of the drift in displacements at the various stations are shown following the release of initial conditions which had been set at zero.

For operational amplifiers which are not drift stabilized the drift of a free-free beam circuit of 8-cells or more can cause considerable difficulty, since the voltage outputs may increase to saturation by the time

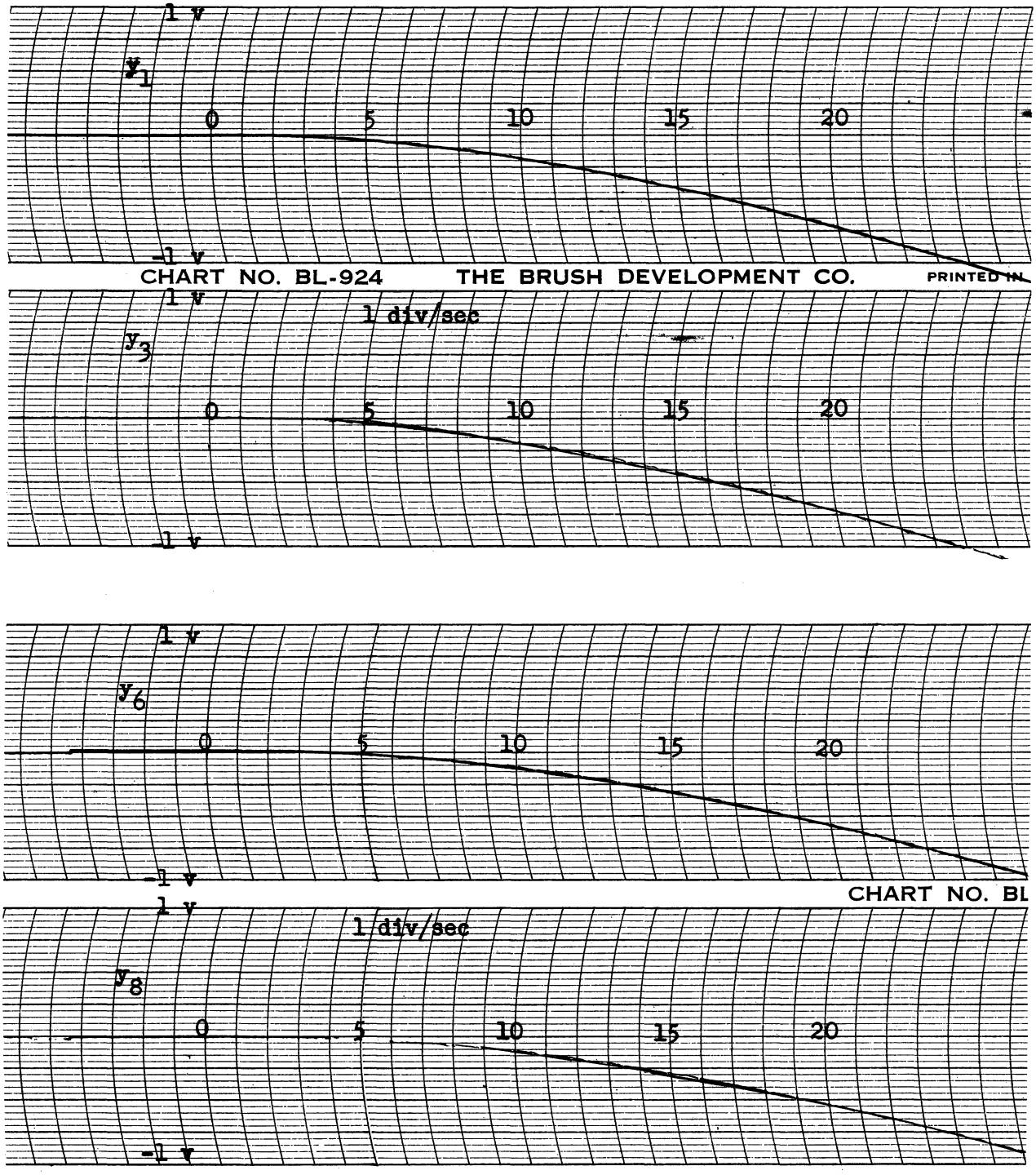

Figure 7-2

Drift of an 8-Cell Free-Free Beam

Following Release of Zero Initial Conditions

several periods of oscillation of the fundamental mode take place. However, with drift stabilized amplifiers the drift effects are fairly small, as can be seen in Figure 7-1. There the biggest displacement represents about a 1 volt drift after 8 periods of the fundamental mode.

In Chapter 10 we will again consider the free-free beam, but with deflection due to transverse shear included in the equations.

CHAPTER 8

BEAMS WITH VISCOUS DAMPING

8.1 Beam Equations Including Viscous Damping

We now take up the problem of flexural vibration of beams when viscous damping is present. The damping will add an additional transverse force proportional to the transverse velocity $\partial y/\partial t$. Thus from Equation (1-1) the new equation becomes

$$\frac{\partial^2}{\partial \bar{x}^2} EI(\bar{x}) \frac{\partial^2 y}{\partial \bar{x}^2} + c(\bar{x}) \frac{\partial y}{\partial \bar{t}} + \rho(\bar{x}) \frac{\partial^2 y}{\partial \bar{t}^2} = \bar{f}(\bar{x}, \bar{t}) \qquad (8\text{-}1)$$

where $c(\bar{x})$ represents the damping force per unit length per unit transverse velocity. Similar to the way in which $EI(\bar{x})$ and $\rho(\bar{x})$ were rewritten in Equations (1-10) and (1-11) as constant factors times dimensionless functions of x, we write

$$c(\bar{x}) = c_o \phi_v(\bar{x}) \qquad (8\text{-}2)$$

Here c_o is equal to the maximum value of $c(\bar{x})$ and $\phi_v(\bar{x})$ is dimensionless. Also we introduce the dimensionless distance variable

$$x = \frac{\bar{x}}{L} \qquad (1\text{-}8)$$

and the dimensionless time variable

$$t = \frac{1}{L^2} \sqrt{\frac{EI_o}{\rho_o}}\, \bar{t} \qquad (1\text{-}13)$$

so that Equation (8-1) becomes

$$\frac{\partial^2}{\partial x^2} \phi_f(x) \frac{\partial^2 y}{\partial x^2} + \frac{L^2 c_o}{\sqrt{\rho_o EI_o}} \phi_v(x) \frac{\partial y}{\partial t} + \phi_d(x) \frac{\partial^2 y}{\partial t^2} = \frac{L^4}{EI_o} \bar{f}(x, t) \qquad (8\text{-}2)$$

Letting

$$c_v = \frac{L^2 c_o}{\sqrt{\rho_o E I_o}} \tag{8-3}$$

and

$$f(x,t) = \frac{L^4}{EI_o} \bar{f}(x,t) \tag{1-16}$$

we have finally

$$\frac{\partial^2}{\partial x^2} \phi_f(x) \frac{\partial^2 y}{\partial x^2} + c_v \phi_v(x) \frac{\partial y}{\partial t} + \phi_d(x) \frac{\partial^2 y}{\partial t^2} = f(x,t) \tag{8-4}$$

For a cantilever beam the end conditions require that

$$y(o,t) = \frac{\partial y}{\partial x}(o,t) = 0 \tag{8-5}$$

and

$$\phi_f(1) \frac{\partial^2 y}{\partial x^2}(1,t) = \frac{\partial}{\partial x} \phi_f(1) \frac{\partial^2 y}{\partial x^2}(1,t) = 0 \tag{8-6}$$

Equation (8-4) is of course subject to initial conditions

$$y(x,o) = Y(x) \tag{1-6}$$

and

$$\frac{\partial y(x,o)}{\partial t} = \dot{Y}(x) \tag{8-7}$$

8.2 Difference Equations Including Viscous Damping

As before we consider the beam displacement y only at certain stations in x. Defining a new distance variable χ such that the distance $\Delta\chi$ between stationsis unity, we have for the bending moment at the nth station

$$m_n = \phi_{f_n}(y_{n+1} - 2y_n + y_{n-1}) \qquad (2\text{-}10)$$

From Equation (8-4) the difference equation at the nth cell becomes

$$\phi_{d_n} \frac{d^2 y_n}{d\tau^2} + c\phi_{v_n} \frac{dy_n}{d\tau} = - m_{n+1} + 2m_n - m_{n-1} + \Phi_n(\tau) \qquad (8\text{-}8)$$

where

$$\Phi_n(\tau) = \frac{1}{N^4} f_n(\tau) \quad , \qquad (8\text{-}9)$$

$$c = \frac{c_v}{N^2} \quad , \qquad (8\text{-}10)$$

and

$$\tau = N^2 t \quad , \qquad (2\text{-}5)$$

N being the number of cells into which the beam is divided.

For an N-cell cantilever beam having a built-in end at $\chi = 1/2$ and a free end at $\chi = N + 1/2$, the complete equations, including viscous damping, are similar to those given in Equations (2-12) and (2-13) except for the addition of the damping term $\phi_{v_n} dy_n/d\tau$ at each cell.

8.3 Computer Circuit for the Viscous-Damping Case

The electronic differential analyzer circuit at the nth cell when viscous damping is included is shown in Figure 8-1. The circuit at the beam ends is similar to those shown in Figures 3-2 and 3-5.

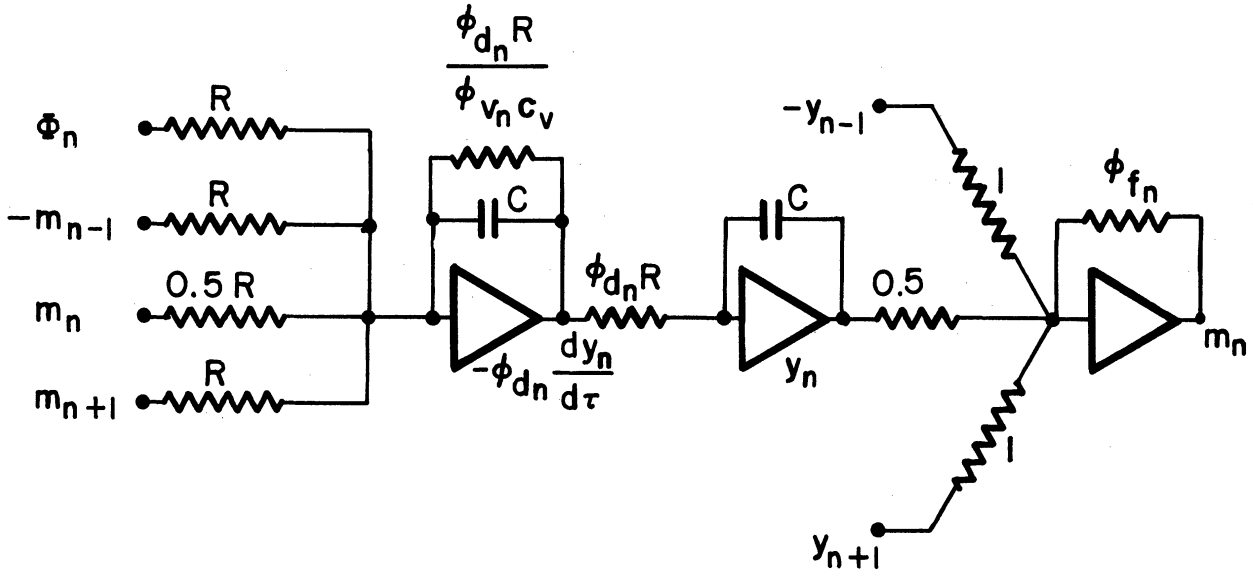

Figure 8-1
Analyzer Circuit at the nth Cell Including Viscous Damping

8.4 Impulse Response of an 8-Cell Cantilever Beam with Viscous Damping

As an actual example of a beam problem including viscous damping, consider a uniform 8-cell cantilever beam with an impulse $\delta(\tau)$ of unit area applied at each station along the beam. An integrator time scale of 0.2 seconds was used for the computer circuit (R = 0.2 megohms, C = 1 microfarad). A 50 volt input pulse of 0.2 seconds duration was applied through 5 megohm input resistors to each of the stations.

In Figures 8-2 and 8-3 the unit impulse response at each station is shown for various damping constants c_v. The results have been normalized for a beam of unit length, and the time scale is given in units of the dimensionless variable t. If $W_n(t)$ represents the unit impulse response at the nth station, then the response y_n at the nth station to any uniform input f(t) is given by

$$y_n(t) = \int_{-\infty}^{t} W_n(t - \sigma) f(\sigma) d\sigma \qquad (8\text{-}8)$$

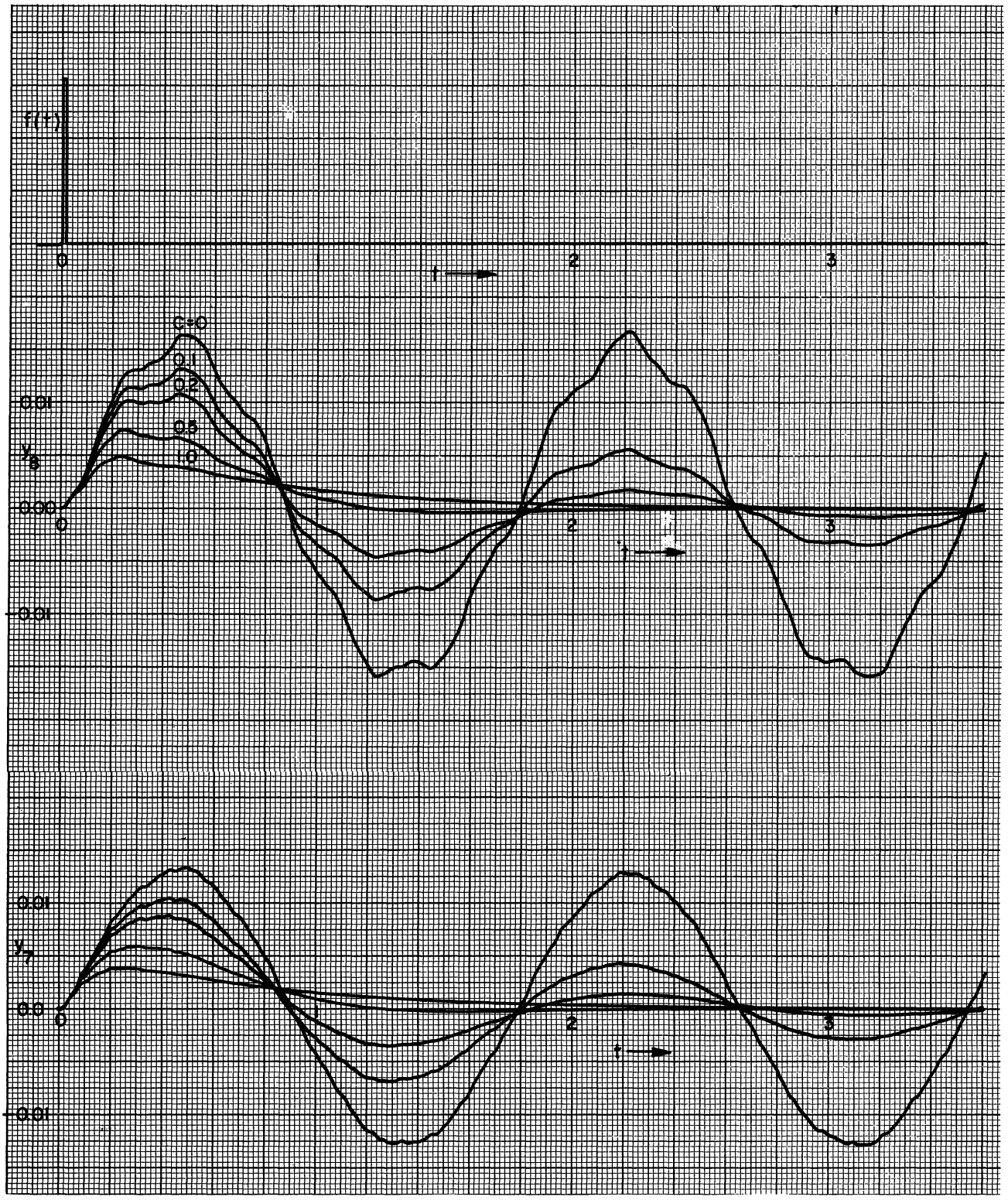

Figure 8-2

Unit Impulse Response of a Uniform Cantilever Beam with Viscous Damping (Input and Displacement at Stations 7 and 8)

Figure 8-3

Unit Impulse Response of a Uniform Cantilever Beam with Viscous Damping (Displacement at Stations 2, 3, 4, 5, and 6)

or the equivalent expression

$$y_n(t) = \int_0^\infty W_n(\sigma) f(t - \sigma) d\sigma \qquad (8\text{-}9)$$

Both these integrals can be approximated conveniently by finite summations. If a differential analyzer of sufficient capacity is available, however, a direct solution with f(t) as the input would be the most practical method of obtaining the beam response.

CHAPTER 9

BEAMS WITH TIME-VARYING BOUNDARY CONDITIONS

9.1 Method of Introducing Time-Varying Boundary Conditions

Up to now we have considered only homogeneous boundary conditions in treating vibrating-beam problems. Actually there is no reason for limiting the solutions to this type of problem. Any non-zero time-varying boundary condition can be introduced. For example, suppose that a beam has its displacement at one end given by an explicit time function. One other condition at this end must also be given; let us assume that the bending moment vanishes. If the end occurs at the nth station, then the difference equations up to the time-varying boundary become

$$\phi_{d_{N-2}} \frac{d^2 y_{N-2}}{d\tau^2} = - m_{N-1} + 2m_{N-2} - m_{N-3} + \Phi_{N-2}(\tau) \qquad (9\text{-}1)$$

$$\phi_{d_{N-1}} \frac{d^2 y_{N-1}}{d\tau^2} = 2m_{N-1} - m_{N-2} + \Phi_{N-1}(\tau)$$

and

$$m_{N-2} = \phi_{f_{N-2}} (y_{N-1} - 2y_{N-2} + y_{N-3}) \qquad (9\text{-}2)$$

$$m_{N-1} = \phi_{f_{N-1}} \left[y_N(\tau) - 2y_{N-1} + y_{N-2} \right]$$

where $y_N(\tau)$ is the specified displacement at the end of the beam.

9.2 Cantilever Beam with Specified Displacement at the Free End.

Assume the beam with the specified displacement at the Nth station is built in at the other end, i.e., $y_o = y_1 = 0$. Equations (2-12) and (2-13)

give the difference equations at the built-in end. Equations (9-1) and (9-3) give the difference equations at the forced end.

An 8-cell uniform cantilever beam with the free end forced was set up on the electronic differential analyzer. As a specific example the prescribed motion $y_N(\tau)$ at the free end was taken as sinusoidal. Other function-generating equipment could have been used to simulate any arbitrary time-varying boundary conditions.[2,10] Note that the beam length is N-1/2 since the end occurs at station N, and not station N+1/2 as is the case for completely free boundary conditions.

9.3 Beam on Elastic Foundations

Consider next the beam shown in Figure 9-1.

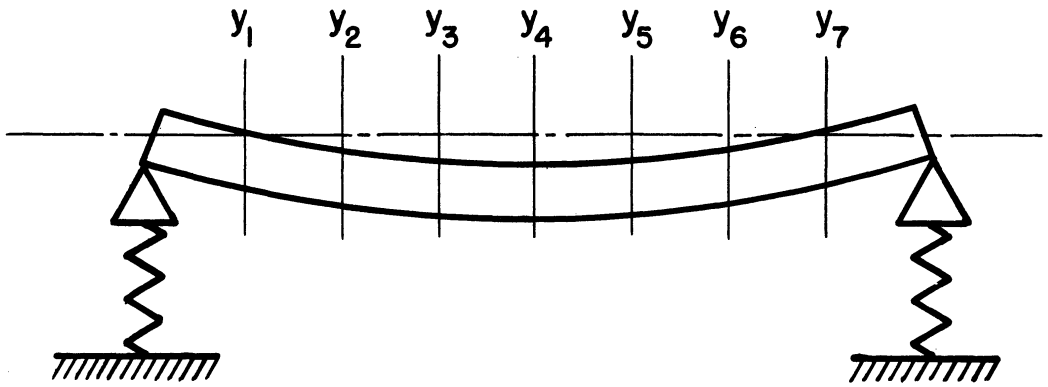

Figure 9-1

Hinged-Hinged Beam on Elastic Supports

Here the ends of the beam are supported elastically and in such a manner that the bending moment vanishes. If the right-hand end occurs at χ = N, the equation of motion at station N-1 is from Equation (2-11)

$$\phi_{d_{N-1}} \frac{d^2 y_{N-1}}{d\tau^2} \doteq 2m_{N-1} - m_{N-2} + \Phi_n(\tau) \qquad (9\text{-}3)$$

while at station N

$$\phi_{d_N} \frac{d^2 y_N}{d\tau^2} = - k\, y_N \qquad (9\text{-}4)$$

where k is the spring constant of the elastic supports. The bending moments m_n are given as usual by Equation (2-10).

CHAPTER 10

VIBRATION OF BEAMS INCLUDING DEFLECTION DUE TO TRANSVERSE SHEAR

10.1 Equations for Transverse Beam Motion, Including Shear Displacements

In Section 1.1 the basic dynamic equation for transverse displacement of a thin beam was given as

$$\frac{\partial}{\partial \bar{x}} V(\bar{x}, \bar{t}) + \rho(\bar{x}) \frac{\partial^2 y(\bar{x}, \bar{t})}{\partial \bar{t}^2} = \bar{f}(\bar{x}, \bar{t}) \tag{10-1}$$

where the shear force $V(x, t)$ is given by

$$V = \frac{\partial}{\partial \bar{x}} M \tag{10-2}$$

The bending moment $M(x, t)$ is given in turn by

$$M = EI(x) \frac{\partial \beta}{\partial \bar{x}} \tag{10-3}$$

where $\beta(\bar{x}, \bar{t})$ is the neutral-axis slope due to the bending-moment. In the thin-beam theory used up to now, the neutral-axis slope due to transverse shear force is neglected, so that $\beta = \partial y / \partial \bar{x}$. However, a more accurate expression for the neutral-axis slope includes both the contribution β due to the bending moment and the contribution α due to the transverse shear force. Thus

$$\frac{\partial y}{\partial x} = \beta + \alpha \tag{10-4}$$

where

$$\alpha = - \frac{V}{kAG(x)} \tag{10-5}$$

Here $kAG(\bar{x})$ is the shear rigidity at $\bar{x}$. From Equations (10-2), (10-3), (10-4), and (10-5)

$$M = EI(\bar{x}) \frac{\partial^2 y}{\partial \bar{x}^2} + \frac{1}{kAG(\bar{x})} \frac{\partial^2 M}{\partial \bar{x}^2} \tag{10-6}$$

and

$$\frac{\partial^2 M}{\partial \bar{x}^2} + \rho(\bar{x}) \frac{\partial^2 y}{\partial \bar{x}^2} = \bar{f}(\bar{x}, \bar{t}) \tag{10-7}$$

become the equations to be solved when transverse shear effects are included.

Similar to the way in which $EI(\bar{x})$ and $\rho(\bar{x})$ were written in Equations (1-10) and (1-11) as constant factors time dimensionless functions of x, we write

$$kAG(\bar{x}) = kAG_o \, \phi_s(\bar{x}) \tag{10-8}$$

where kAG_o is equal to the maximum value of $kAG(\bar{x})$ and where $\phi_s(\bar{x})$ is dimensionless. As before we introduce the dimensionless distance variable

$$x = \frac{\bar{x}}{L} \tag{1-8}$$

and the dimensionless time variable

$$t = \frac{1}{L^2} \sqrt{\frac{EI_o}{\rho_o}} \, \bar{t} \tag{1-13}$$

We also define a parameter S given by

$$S = \frac{EI_o}{kAG_o L^2} \tag{10-9}$$

From Equations (1-8), (1-13), and (10-9) Equations (10-6) and (10-7) become

$$\frac{\partial^2 \bar{M}}{\partial x^2} + \phi_d(x) \frac{\partial^2 y}{\partial t^2} = f(x, t) \tag{10-10}$$

where

$$\bar{M} = \phi_f(x) \frac{\partial^2 y}{\partial x^2} + \frac{S}{\phi_s(x)} \frac{\partial^2 \bar{M}}{\partial x^2} \tag{10-11}$$

and where

$$f(x, t) = \frac{L^4}{EI_o} \bar{f}(x, t) \tag{1-16}$$

The parameter S represents the relative importance of the deflection due to transverse shear, and for a given beam cross-section is inversely proportional to the beam length squared.

10.2 Difference Equations Including the Transverse Shear Effects

Next we divide the beam length into N segments and consider the displacement y only at stations in x. Defining a new distance variable χ such that the distance $\Delta\chi$ between stations is unity, we have for the equation of motion at the nth cell

$$\phi_{d_n} \frac{d^2 y_n}{d\tau^2} = - m_{n+1} + 2m_n - m_{n-1} + \Phi_n(\tau) \tag{10-12}$$

where from Section 2.1

$$\tau = N^2 t \tag{2-5}$$

and

$$\Phi_n(\tau) = \frac{1}{N^4} f_n(\tau) \tag{10-13}$$

From Equation (10-11) it follows that m_n is given by

$$m_n = \phi_{f_n}(y_{n+1} - 2y_n + y_{n-1}) + \frac{SN^2}{\phi_{s_n}}(m_{n+1} - m_n + m_{n-1}) \quad (10\text{-}14)$$

The electronic differential analyzer circuit for solving Equation (10-14) at the nth cell is shown in Figure 10-1. Note that there is now a feedback loop in which these are no integrators. In order to avoid possible electronic instabilities (high frequency oscillations) whenever ϕ_{s_n}/SN^2 becomes too small, a small capacitor is inserted across the feedback resistor in amplifier A_6. This capacitor is sufficient to reduce the gain of the $A_4 - A_5 - A_6$ loop well below unity at those frequencies where the gain of the dc amplifiers proper is the order of unity (about 10 kc). The capacitor is, however, small enough so that it does not materially affect the accuracy of the computation, which involves frequencies of the order of 1 cps or lower. Note that in any case amplifier A_6 with this additional feedback capacitor is only involved in computing the correction to the beam curvature as a result of transverse shear forces. The main loop ($A_1 - A_2 - A_3 - A_4 - A_5$) is not affected.

Boundary conditions for the beam including transverse shear are the same as those used previously. For a free end at $\chi = N + 1/2$ the end condition requires that $m_N = m_{N+1} = 0$. For a built-in end at $\chi = N+1/2$, $y_N = y_{N+1} = 0$. For a hinged end at $\chi = N$, $y_N = m_N = 0$.

An 8-cell uniform free-free beam was set up on the electronic differential analyzer using an integrator time scale of 0.2 seconds. Normal-mode frequencies were obtained for 1/S equal to 640, 320, 160, 64, and 32. These correspond to length to thickness ratios of approximately 15, 10.5, 7.5, 4.7, and 3.3 respectively for a rectangular steel beam. The percentage deviation from the mode frequency for an infinitely thin beam ($1/S = \infty$) was in each case compared with analyzer solutions for a continuous free-free beam, including transverse shear effects.[2] The results are presented in Figure 10-2 which shows a plot of β_s/β versus 1/S for the first three modes, where β_s is the normal-mode frequency including transverse shear, and where β

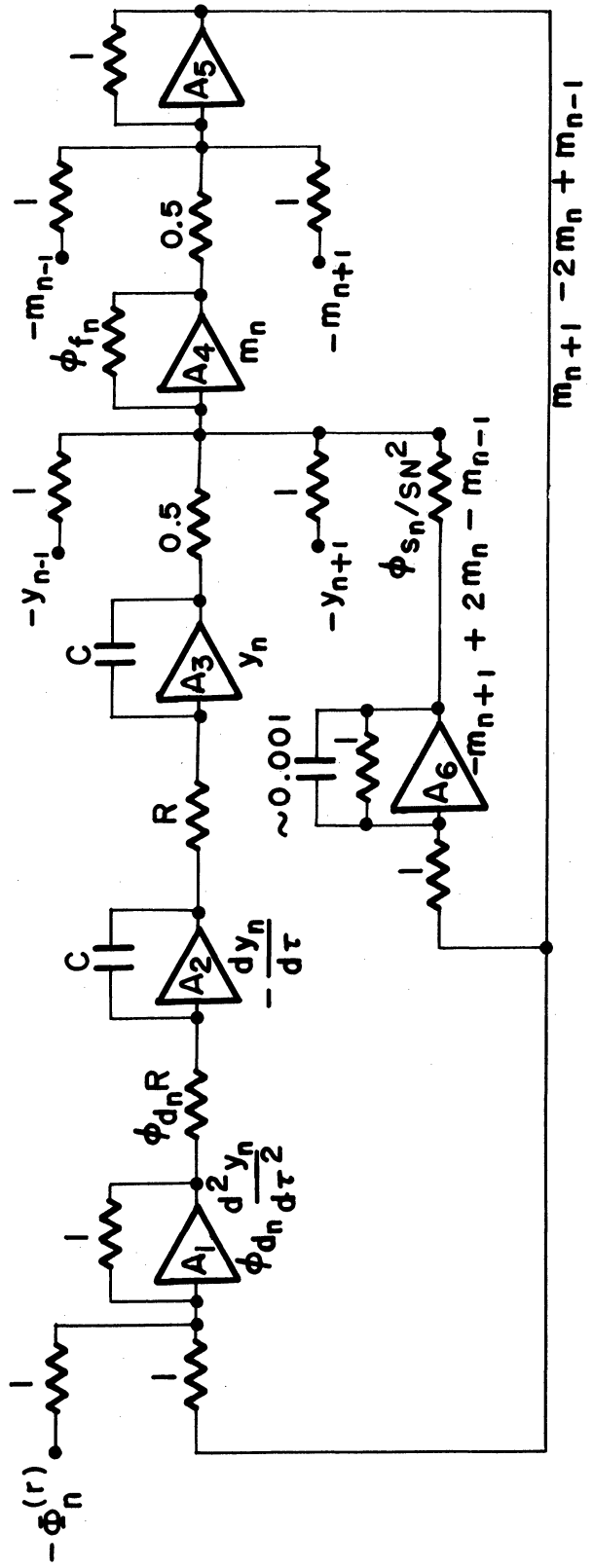

Figure 10-1 Analyzer Circuit for Transverse Beam Displacement at the nth Station, Including Transverse Shear

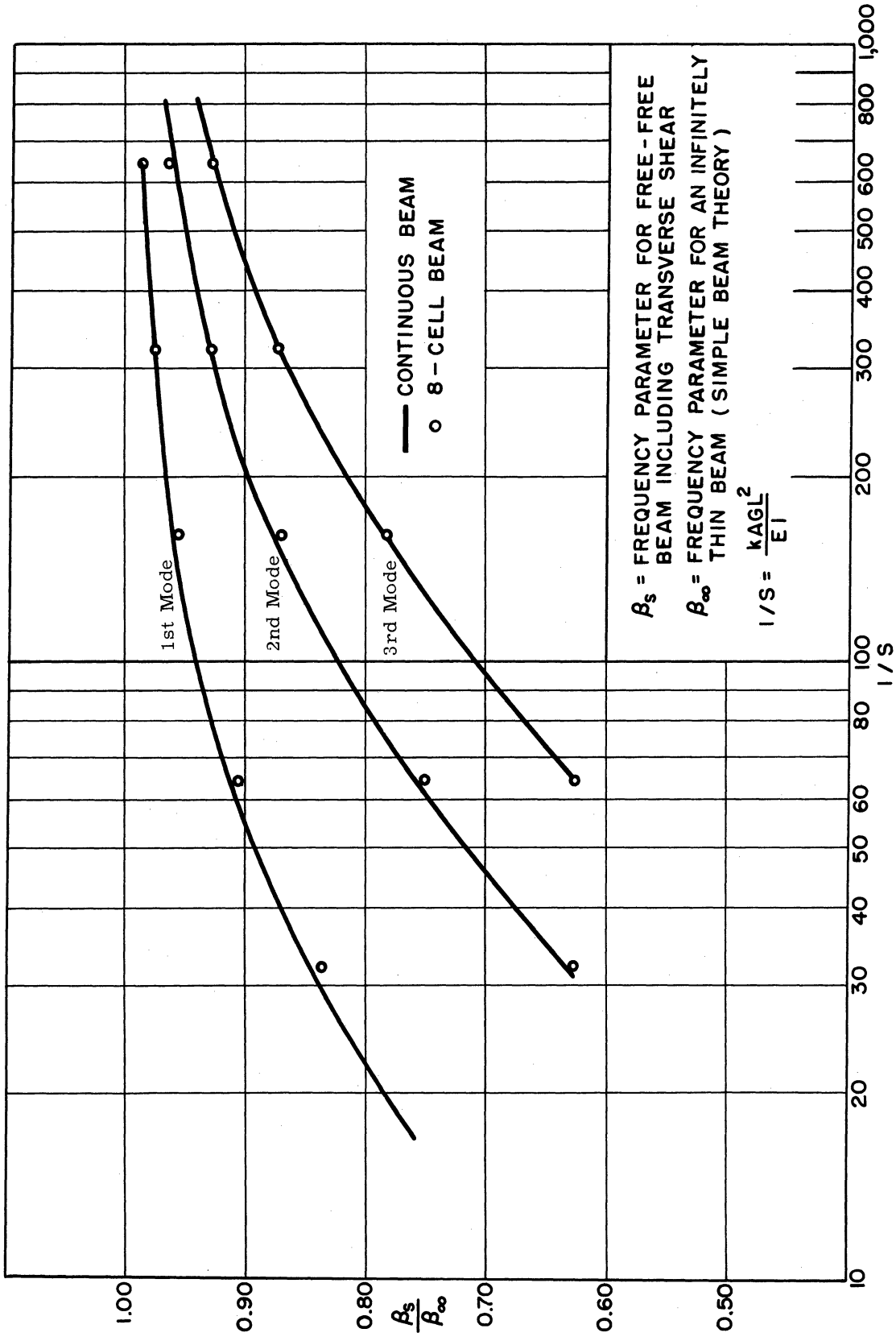

Figure 10-2 Comparison of Transverse Shear Effect on Normal-Mode Frequency for a Uniform Free-Free Beam

is the frequency when the transverse shear is neglected (simple beam theory). The correlation is apparently quite good, indicating that it is very practical to consider effects of transverse shear when solving beam problems by the difference method.

APPENDIX I

CALCULATION OF MODE FREQUENCIES AND SHAPES FOR CELLULAR FREE-FREE BEAMS

Equations to be Solved

From Equations (2-10) and (2-11) and the boundary conditions in Table I, Section 2.2, we can obtain a set of N simultaneous ordinary differential equations for a uniform free-free beam. If we further make the assumption that the displacement y_i at the ith station varies as sin $\lambda\tau$, the time variable τ is eliminated from the equations and we have

$$(1-\lambda^2)y_1 - 2y_2 + y_3 = 0 \qquad \text{(A-1)}$$

$$-2y_1 + (5-\lambda^2)y_2 - 4y_3 + y_4 = 0 \qquad \text{(A-2)}$$

$$y_1 - 4y_2 + (6-\lambda^2)y_3 - 4y_4 + y_5 = 0 \qquad \text{(A-3)}$$

$$y_2 - 4y_3 + (6-\lambda^2)y_4 - 4y_5 + y_6 = 0 \qquad \text{(A-4)}$$

. . . . . .

. . . . . .

. . . . . .

$$y_{N-5} - 4y_{N-4} + (6-\lambda^2)y_{N-3} - 4y_{N-2} + y_{N-1} = 0 \qquad \text{(A-5)}$$

$$y_{N-4} - 4y_{N-3} + (6-\lambda^2)y_{N-2} - 4y_{N-1} + y_N = 0 \qquad \text{(A-6)}$$

$$y_{N-3} - 4y_{N-2} + (5-\lambda^2)y_{N-1} - 2y_N = 0 \qquad \text{(A-7)}$$

$$y_{N-2} - 2y_{N-1} + (1-\lambda^2)y_N = 0 \qquad \text{(A-8)}$$

Here the y_i's are no longer functions of time but represent the amplitude of the normal-mode oscillation of frequency λ. The above N

simultaneous algebraic equations have a non-trivial solution only if the determinant of the coefficients vanishes. The determinant, when expanded, becomes a polynomial in λ^2 of order N. The roots of the polynomial represent the normal-mode frequencies for the uniform N-cell free-free beam.

Determination of the Characteristic Equations for the Mode Frequencies

The Nth order polynomial in λ^2 representing the characteristic equation for the N-cell free-free beam is apparently impossible to obtain in the general N-cell case. Thus the polynomial must be found by resolving Equations (A-1), (A-2), ..., for each number of cells desired. One way to solve the equations is to find y_3 in terms of y_1 and y_2 from Equation (A-1). Thus

$$y_3 = (-1 + \lambda^2)y_1 + 2y_2 \qquad \text{(A-9)}$$

From (A-2) and (A-9)

$$y_4 = (-2 + 4\lambda^2)y_1 + (-3 - \lambda^2)y_2 \qquad \text{(A-10)}$$

Similarly

$$y_5 = (-3 + 9\lambda^2 + \lambda^4)y_1 + (4 + 6\lambda^2)y_2 \qquad \text{(A-11)}$$

$$y_6 = (-4 + 14\lambda^2 + 8\lambda^4)y_1 + (5 + 21\lambda^2 + \lambda^4)y_2 \qquad \text{(A-12)}$$

$$y_7 = (-5 + 14\lambda^2 + 35\lambda^4 + \lambda^6)y_1 + (6 + 56\lambda^2 + 10\lambda^4)y_2 \qquad \text{(A-13)}$$

$$y_8 = (-6 + 110\lambda^4 + 12\lambda^6)y_1 + (7 + 126\lambda^2 + 55\lambda^4 + \lambda^6)y_2 \qquad \text{(A-14)}$$

and so on. When the other end of the beam is reached Equations (A-7) and (A-8) are used to determine two final equations involving only y_1 and y_2. Thus for an 8-cell beam the final two equations are

$$y_5 - 4y_6 + (5 - \lambda^2)y_7 - 2y_8 = 0 \qquad \text{(A-15)}$$

and

$$y_6 - 2y_7 + (1 - \lambda^2)y_8 = 0 \qquad \text{(A-16)}$$

Equations (A-11), (A-12), (A-13), and (A-14) are used to eliminate y_5, y_6, y_7, and y_8 from Equations (A-15) and (A-16), from which

$$(28\lambda^2 - 90\lambda^4 - 54\lambda^6 - \lambda^8)y_1 + (-56\lambda^2 - 120\lambda^4 - 12\lambda^6)y_2 = 0 \qquad \text{(A-17)}$$

and

$$(-8\lambda^2 + 48\lambda^4 - 100\lambda^6 - 12\lambda^8)y_1 + (28\lambda^2 - 90\lambda^4 - 54\lambda^6 - \lambda^8)y_2 = 0 \qquad \text{(A-18)}$$

Eliminating y_1 and y_2 from Equations (A-17) and (A-18) we have finally

$$-336\lambda^4 + 3312\lambda^6 - 5140\lambda^8 + 2432\lambda^{10} - 456\lambda^{12} + 36\lambda^{14} - \lambda^{16} = 0 \qquad \text{(A-19)}$$

This is the characteristic equation for an 8-cell free-free beam.

Calculation of the Normal-Mode Frequencies

The solutions (roots of the polynomial) of Equation (A-19) are the normal-mode frequencies for the 8-cell beam. Note that we have a second order root when $\lambda^2 = 0$. This corresponds to a constant displacement or constant velocity of the free-free beam in translation or rotation. The next four roots of Equation (A-19) are

$$\lambda_1^2 = 0.12391 \quad , \quad \lambda_1 = 0.35201$$

$$\lambda_2^2 = 0.88046 \quad , \quad \lambda_2 = 0.93833$$

$$\lambda_3^2 = 2.95610 \quad , \quad \lambda_3 = 1.71933$$

$$\lambda_4^2 = 6.54684 \quad , \quad \lambda_4 = 2.55868$$

These represent the frequencies for the first four modes of oscillation of a uniform 8-cell free-free beam. Since ΔX , the distance between stations, is unity, the length of our 8-cell beam is 8. To find the frequency for a beam of unit length we need to multiply the above frequencies by 8^2 or 64. These frequencies can then be compared with those given in Table II of Section 4.3 for a continuous free-free beam. This has been done in the Table XI below.

TABLE XI

Comparison of Frequency Parameter β for
Continuous and 8-Cell Free-Free Beams

Mode	(Continuous Beam)	(8-Cell Beam)	% Difference
1	22.373	22.529	+ 0.72
2	61.673	60.053	- 2.63
3	120.90	110.037	- 9.00
4	199.86	163.756	-18.06

The above calculations were carried out for free-free cellular beams from 3 to 16 cells. However, to simplify the calculations one can take advantage of the symmetry of the uniform free-free beam.

Determination of Symmetrical Mode Frequencies

The first, third, fifth, etc., modes of a uniform free-free beam are symmetrical about the beam center. Thus we can solve for these modes by considering only one half of the beam and by letting the first and third derivatives along the beam vanish at the center. For an 8-cell beam this is equivalent to considering only the displacements y_1, y_2, y_3, and y_4 and letting $y_5 = y_4$ and $y_6 = y_3$. From Equations (A-1) through (A-4) it follows that

$$(1- \lambda^2)y_1 - 2y_2 + y_3 = 0 \qquad \text{(A-20)}$$

$$-2y_1 + (5-\lambda^2)y_2 - 4y_3 + y_4 = 0 \qquad \text{(A-21)}$$

$$y_1 - 4y_2 + (6-\lambda^2)y_3 - 3y_4 = 0 \qquad \text{(A-22)}$$

$$y_2 - 3y_3 + (2-\lambda^2)y_4 = 0 \qquad \text{(A-23)}$$

From Equations (A-20) through (A-23) it is easy to eliminate the y's, obtaining

$$-4\lambda^2 + 34\lambda^4 - 14\lambda^6 - \lambda^8 = 0 \qquad \text{(A-24)}$$

as the characteristic equation for the symmetrical modes of an 8-cell free-free beam. The first two roots of this equation (other than $\lambda = 0$) will give the λ_1 and λ_3 values found in the previous section. However, Equation (A-21) was much easier to obtain than the complete Equation (A-19) and the roots are simpler to calculate. The saving in computation time is particularly helpful when the solutions for N up to 16 are calculated.

For an odd number of cells N the symmetrical modes are obtained by considering $\frac{N+1}{2}$ cells and letting

$$y_{\frac{N+1}{2}-1} = y_{\frac{N+1}{2}+1}, \quad y_{\frac{N+1}{2}-2} = y_{\frac{N+1}{2}+2}$$

Determination of Anti-Symmetrical Mode Frequencies

The second, fourth, sixth, etc., modes of a uniform free-free beam are antisymmetrical with respect to the beam center. Thus we can solve for these modes too by considering only one-half of the beam and by letting the zeroth and second derivatives along the beam vanish at the center. For an odd number of cells N this is equivalent to letting $y_{\frac{N+1}{2}} = 0$ and $y_{\frac{N+1}{2}-1} = -y_{\frac{N+1}{2}+1}$. For an even number of cells $y_{\frac{N}{2}} = -y_{\frac{N}{2}+1}$ and $y_{\frac{N}{2}-1} = -y_{\frac{N}{2}+2}$. Thus for an 8-cell beam $y_4 = -y_5$ and $y_3 = -y_6$. From Equations (A-1) through (A-9) it follows that

$$(1-\lambda^2)y_1 - 2y_2 + y_3 = 0 \qquad \text{(A-25)}$$

$$-2y_1 + (5-\lambda^2)y_2 - 4y_3 + y_4 = 0 \qquad \text{(A-26)}$$

$$y_1 - 4y_2 + (6-\lambda^2)y_3 - 5y_4 = 0 \qquad \text{(A-27)}$$

$$y_2 - 5y_3 + (10-\lambda^2)y_4 = 0 \qquad \text{(A-28)}$$

From Equations (A-25) through (A-28) it is again easy to eliminate the y's, obtaining

$$-84\lambda^2 + 114\lambda^4 - 22\lambda^6 + \lambda^8 = 0 \qquad \text{(A-29)}$$

as the characteristic equation for the anti-symmetrical modes of an 8-cell free-free beam. The first two roots of Equation (A-29) (other than $\lambda = 0$) will give the λ_2 and λ_4 values found in the previous section. In fact Equations (A-24) and (A-29) for the symmetrical and anti-symmetrical modes respectively are the factors of Equation (A-19). Thus

$$-336\lambda^4 + 3312\lambda^6 - 5140\lambda^8 + 2432\lambda^{10} - 456\lambda^{12} + 36\lambda^{14} - \lambda^{16} =$$

$$(-4\lambda^2+34\lambda^4-14\lambda^6-\lambda^8)(-84\lambda^2+114\lambda^4-22\lambda^6+\lambda^8) = 0 \qquad \text{(A-30)}$$

is the complete characteristic equation for the 8-cell uniform free-free beam.

Normal-Mode Frequencies for 3 Cells through 16 Cells

Using the techniques described in the previous two sections the normal-mode frequencies for the first four modes of a uniform free-free beam were calculated for 3 cells up to 16 cells. The resulting dimensionless frequency parameters are compared with the continuous beam in Table XII.

TABLE XII

Comparison of Frequency Parameter β for
Continuous and Cellular Uniform Free-Free Beams

First Mode

No. of Cells		% Error
3	22.045	-1.47
4	22.627	1.17
5	22.654	1.25
6	22.610	1.07
7	22.565	0.90
8	22.529	0.72
9	22.501	0.58
10	22.479	0.46
11	22.462	0.41
12	22.449	0.36
14	22.430	0.26
16	22.417	0.20
Continuous	22.373	--

Second Mode

No. of Cells		% Error
4	50.596	-17.95
5	55.902	- 9.36
6	58.214	- 5.61
7	59.387	- 3.70
8	60.053	- 2.63
9	60.465	- 1.96
10	60.737	- 1.51
11	60.925	- 1.21
12	61.061	- 0.99
13	61.163	- 0.82
15	61.302	- 0.60
Continuous	61.673	--

Third Mode

No. of Cells		% Error
5	87.25	-27.84
6	99.28	-17.89
7	105.99	-12.34
8	110.04	- 9.00
9	112.64	- 6.84
10	114.41	- 5.37
11	115.66	- 4.34
12	116.58	- 3.58
14	117.81	- 2.56
16	118.58	- 1.92
Continuous	120.90	--

Fourth Mode

No. of Cells		% Error
6	131.71	-34.01
7	151.28	-24.30
8	163.76	-18.06
9	172.07	-13.90
10	177.84	-11.01
11	182.00	- 8.93
12	185.09	- 7.39
13	187.43	- 6.21
15	190.71	- 4.57
Continuous	199.86	--

Summary of Characteristic Equations

The characteristic equations for the mode frequencies are given for 3 through 16 cells in the following table:

TABLE XIII

Characteristic Equations for a Uniform
Cellular Free-Free Beam

Three Cells

$$6\lambda^4 - \lambda^6 = 0$$

Four Cells

$$20\lambda^4 - 12\lambda^6 + \lambda^8 = (2\lambda^2 - \lambda^4)(10\lambda^2 - \lambda^4) = 0$$

Five Cells

$$50\lambda^4 - 75\lambda^6 + 18\lambda^8 - \lambda^{10} = (5\lambda^2 - \lambda^4)(10\lambda^2 - 13\lambda^4 + \lambda^6) = 0$$

Six Cells

$$105\lambda^4 - 328\lambda^6 + 166\lambda^8 - 24\lambda^{10} + \lambda^{12} = (3\lambda^2 - 8\lambda^4 + \lambda^6)(35\lambda^2 - 16\lambda^4 + \lambda^6) = 0$$

Seven Cells

$$196\lambda^4 - 1134\lambda^6 + 1050\lambda^8 - 293\lambda^{10} + 30\lambda^{12} - \lambda^{14} =$$

$$(14\lambda^2 - 11\lambda^4 + \lambda^6)(14\lambda^2 - 70\lambda^4 + 19\lambda^6 - \lambda^8) = 0$$

Eight Cells

$$336\lambda^4 - 3312\lambda^6 + 5140\lambda^8 - 2432\lambda^{10} + 456\lambda^{12} - 36\lambda^{14} + \lambda^{16} =$$

$$(4\lambda^2 - 34\lambda^4 + 14\lambda^6 - \lambda^8)(84\lambda^2 - 114\lambda^4 + 22\lambda^6 - \lambda^8) = 0$$

Nine Cells

$$540\lambda^4 - 8514\lambda^6 + 20814\lambda^8 - 15471\lambda^{10} + 4690\lambda^{12} - 655\lambda^{14} + 42\lambda^{16} - \lambda^{18} =$$

$$(30\lambda^2 - 63\lambda^4 + 17\lambda^6 - \lambda^8)(18\lambda^2 - 246\lambda^4 + 167\lambda^6 - 25\lambda^8 + \lambda^{10}) = 0$$

Ten Cells

$$825\lambda^4-19800\lambda^6+72722\lambda^8-80584\lambda^{10}+36771\lambda^{12}-8040\lambda^{14}+890\lambda^{16}-48\lambda^{18}+\lambda^{20}=$$

$$(5\lambda^2-104\lambda^4+101\lambda^6-20\lambda^8+\lambda^{10})(165\lambda^2-528\lambda^4+229\lambda^6-28\lambda^8+\lambda^{10})=0$$

Eleven Cells

$$1210\lambda^4-42471\lambda^6+225654\lambda^8-358435\lambda^{10}+234696\lambda^{12}-74980\lambda^{14}+12698\lambda^{16}$$
$$-1161\lambda^{18}+54\lambda^{20}-\lambda^{22}=$$

$$(55\lambda^2-253\lambda^4+148\lambda^6-23\lambda^8+\lambda^{10})(22\lambda^2-671\lambda^4+957\lambda^6-300\lambda^8+31\lambda^{10}$$
$$-\lambda^{12})=0$$

Twelve Cells

$$1716\lambda^4-85228\lambda^6+634985\lambda^8-1401600\lambda^{10}+1271536\lambda^{12}-567192\lambda^{14}+137334\lambda^{16}$$
$$-18880\lambda^{18}+1468\lambda^{20}-60\lambda^{22}+\lambda^{24}=$$

$$(6\lambda^2-259\lambda^4+504\lambda^6-204\lambda^8+26\lambda^{10}-\lambda^{12})(286\lambda^2-1859\lambda^4+1560\lambda^6-380\lambda^8$$
$$+34\lambda^{10}-\lambda^{12})=0$$

Thirteen Cells

$$(91\lambda^2-806\lambda^4+884\lambda^6-269\lambda^8+29\lambda^{10}-\lambda^{12})=0 \text{ (antisymmetrical modes)}$$

Fourteen Cells

$$(7\lambda^2-560\lambda^4+1966\lambda^6-1420\lambda^8+343\lambda^{10}-32\lambda^{12}+\lambda^{14})=0$$
(symmetrical modes)

Fifteen Cells

$$(140\lambda^2-2178\lambda^4+4090\lambda^6-2139\lambda^8+426\lambda^{10}-35\lambda^{12}+\lambda^{14})=0$$
(antisymmetrical modes)

Sixteen Cells

$$(8\lambda^2-1092\lambda^4+6412\lambda^6-7610\lambda^8+3068\lambda^{10}-518\lambda^{12}+38\lambda^{14}-\lambda^{16})=0$$
(symmetrical modes)

Calculation of Mode Shapes

The mode shapes for the cellular free-free beam are readily calculated once the mode frequencies have been found. For example, consider the symmetrical modes of an 8-cell free-free beam. From Equations (A-20) through (A-23) the following two equations are obtained by eliminating y_3 and y_4:

$$(1 - 5\lambda^2 - \lambda^4)y_1 + (-1 - 5\lambda^2)y_2 = 0 \qquad \text{(A-31)}$$

and

$$(-1 + 7\lambda^2 - 4\lambda^2)y_1 + (1 - \lambda^2 - \lambda^4)y_2 = 0 \qquad \text{(A-32)}$$

Indeed, Equation (A-24) is obtained directly from Equations (A-31) and (A-32). In computing the mode shape corresponding to a particular mode frequency the displacement at one of the stations is arbitrary in magnitude; the rest of the displacements are then determined. Let us set y_1 equal to unity. From either Equation (A-31) or (A-32) y_2 can be calculated for a given λ^2. For example, $\lambda^2 = 0.12391$ for the first mode, from which $y_2 = 0.22543$. Once y_1 and y_2 are known, y_3 and y_4 can be calculated from Equations (A-9) and (A-10).

The third-mode displacements are obtained in the same manner by setting $\lambda^2 = 2.95610$. The second and fourth-mode displacements are computed from the antisymmetrical solution. The following table summarizes the calculations.

TABLE XIV

Theoretical Mode Shapes for an 8-Cell Uniform Free-Free Beam

First Mode	Second Mode
$y_1 = 1.0000$	$y_1 = 1.0000$
$y_2 = 0.2254$	$y_2 = -0.5486$
$y_3 = -0.4252$	$y_3 = -1.2167$
$y_4 = -0.8001$	$y_4 = -0.6070$

Third Mode	Fourth Mode
$y_1 = 1.0000$	$y_1 = 1.000$
$y_2 = -1.4270$	$y_2 = -2.328$
$y_3 = -0.8980$	$y_3 = 0.891$
$y_4 = 1.3248$	$y_4 = 1.97$

The mode shapes for the continuous uniform free-free beam can be calculated from the equation[8]

$$y_n(x) = C\left[\sin\sqrt{\beta}_n x + \sinh\sqrt{\beta}_n x + \frac{\sin\sqrt{\beta}_n - \sinh\sqrt{\beta}_n}{-\cos\sqrt{\beta}_n + \cosh\sqrt{\beta}_n}\left(\cos\sqrt{\beta}_n x + \cosh\sqrt{\beta}_n x\right)\right] \qquad \text{(A-33)}$$

Here C is an arbitrary constant. The first two modes are also tabulated by Raleigh.[14] In Figure 4-5 the mode shapes for continuous and 8-cell free-free beams are compared. In each case the cellular mode was matched with the continuous beam at one point.

APPENDIX II

CALCULATION OF MODE FREQUENCIES AND SHAPES FOR CELLULAR CANTILEVER BEAMS

Characteristic Equations

The normal-mode frequencies for a uniform cellular cantilever beam are obtained in the same manner as those for the free-free beam (see Appendix I). It turns out that the characteristic equations which determine the mode-frequencies are almost identical with those given for the free-free beam in Table XIII; the only difference is that the order of the equation in λ^2 is one degree less and a -1 is added to the polynomial. Thus from Table XIII the characteristic equation for a uniform 8-cell free-free beam is given by

$$336\lambda^4 - 3312\lambda^6 + 5140\lambda^8 - 2432\lambda^{10} + 456\lambda^{12} - 36\lambda^{14} + \lambda^{16} = 0$$

while for a uniform 8-cell cantilever beam the characteristic equation is given by

$$-1 + 336\lambda^2 - 3312\lambda^4 + 5140\lambda^6 - 2432\lambda^8 + 456\lambda^{10} - 36\lambda^{12} + \lambda^{14} = 0$$

Here there is no root $\lambda^2 = 0$; all motions are sinusoidal oscillations. This is because the cantilever beam is clamped at one end. It cannot translate or rotate through space like the free-free beam.

Normal-Mode Frequencies

From the characteristic equations the normal-mode frequencies of the uniform cellular cantilever beam can be calculated. When the number of cells becomes large, the frequencies for modes higher than the first are almost identical with those for the free-free beam. We have taken advantage of this to extrapolate cantilever-beam frequencies from free-free beam frequencies in the following table, which compares the frequency parameter β for the cellular cantilever beam with β for a continuous uniform cantilever beam. The first five modes are given for 3 to 16 cells.

TABLE XV

Comparison of Frequency Parameter β for
Continuous and Cellular Uniform Cantilever Beams

First Mode			Second Mode		
No. of Cells	β	% Error	No. of Cells	β	% Error
2	4.000	13.78			
3	3.728	6.03	3	21.728	- 1.36
4	3.634	3.36	4	22.262	1.04
5	3.591	2.13	5	22.289	1.17
6	3.568	1.48	6	22.254	1.02
7	3.554	1.08	7	22.217	0.85
8	3.545	0.83	8	22.144	0.70
9	3.539	0.65	9	22.15	0.55
10	3.535	0.53	10	22.13	0.46
11		0.45	11		0.41
12		0.38	12		0.36
14		0.27	14		0.26
16		0.20	16		0.20
Continuous	3.5160	-	Continuous	22.030	-

Third Mode			Fourth Mode		
No. of Cells	β	% Error	No. of Cells	β	% Error
4	50.628	-17.92			
5	55.939	- 9.33	5	87.24	-27.85
6	58.246	- 5.60	6	99.28	-17.90
7	59.41	- 3.71	7	105.99	-12.34
8	60.06	- 2.56	8	110.04	- 9.00
9	60.46	- 2.01	9	112.64	- 6.84
10	60.74	- 1.56	10	114.41	- 5.37
11	60.93	- 1.25	11	115.66	- 4.34
12	61.06	- 1.04	12	116.58	- 3.58
13	61.16	- 0.87	14	117.81	- 2.56
15	61.30	- 0.65	16	118.58	- 1.92
Continuous	61.698	-	Continuous	120.90	-

TABLE XV (continued)

Fifth Mode

No. of Cells	β	% Error
6	131.71	-34.01
7	151.28	-24.30
8	163.76	-18.06
9	172.07	-13.90
10	177.84	-11.01
11	182.00	- 8.93
12	185.09	- 7.39
13	187.43	- 6.21
15	190.71	- 4.57
Continuous	199.86	-

Mode Shapes

Mode shapes for the cellular cantilever beam are computed in the same manner as those for the free-free beam (see Appendix I). The calculations are somewhat more tedious, however, since symmetry effects cannot be utilized. The mode shapes for the continuous uniform cantilever beam are calculated from the equation[8]

$$y_n(x) = C \left[\cos \sqrt{\beta}_n x - \cosh \sqrt{\beta}_n x - \frac{\cos \sqrt{\beta}_n + \cosh \sqrt{\beta}_n}{\sin \sqrt{\beta}_n + \sinh \sqrt{\beta}_n} (\sin \sqrt{\beta}_n x - \sinh \sqrt{\beta}_n x) \right] \quad \text{(A-34)}$$

where C is an arbitrary constant. In Figure 4-3 the mode shapes for 4 and 8-cell c antilever beams are compared with those for the uniform beam for the first four modes. In each case the cellular and continuous mode shapes were matched at one point.

APPENDIX III

MODE FREQUENCIES AND SHAPES FOR CELLULAR CLAMPED-CLAMPED BEAMS

Normal-Mode Frequencies

Although we have not discussed clamped-clamped beams (both ends built-in) in the main body of the report this type of beam is certainly of interest. The difference equations, characteristic polynomials, and normal-mode frequencies for the uniform clamped-clamped beam can be calculated by the same methods which were used in Appendix I for the free-free beam. It turns out that the characteristic equations and hence the normal-mode frequencies are exactly the same in both cases (except that the clamped-clamped cellular beam has no characteristic roots $\lambda = 0$). Thus the curves in Figure 4-4 which give the percentage deviation in normal-mode frequency as a function of the number of cells for a free-free beam apply equally well to a clamped-clamped beam.

Normal-Mode Shapes

Using the techniques described in Appendix I the normal-mode shapes for the cellular uniform clamped-clamped beam can be calculated. In Figure A-1 the mode shapes for continuous, 5 and 8-cell clamped-clamped beams are compared.

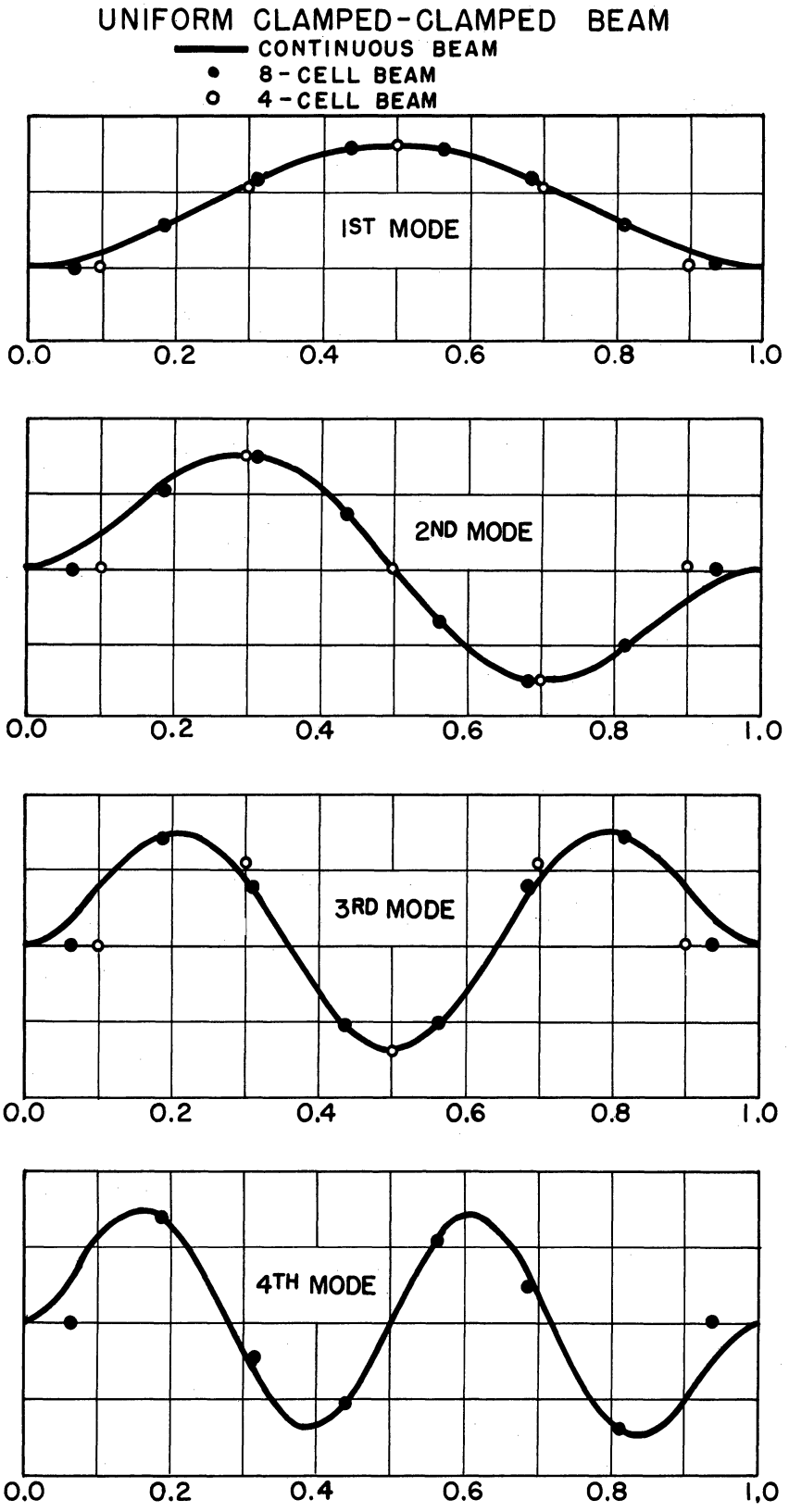

Figure A-1 Comparison of Mode Shapes for Cellular and Continuous Clamped-Clamped Beams

BIBLIOGRAPHY

1. Hagelbarger, Howe and Howe, Investigation of the Utility of an Electronic Analog Computer in Engineering Problems, External Memorandum UMM-28 (April 1, 1949), University of Michigan Engineering Research Institute, AF Con. W33(038)ac-14222 (Project MX-794).

2. Howe, Howe and Rauch, Application of the Electronic Differential Analyzer to the Oscillation of Beams, Including Shear and Rotary Inertia, External Memorandum UMM-67 (January 1951), University of Michigan Engineering Research Institute.

3. Howe, Howe and Rauch, Solution of Linear Differential Equations with Time Varying Coefficients by the Electronic Differential Analyzer, Project Cyclone Symposium II, Part 2, 89 (May 1952).

4. Corcos, Howe, Rauch and Sellars, Application of the Electronic Differential Analyzer to Eigenvalue Problems, Project Cyclone Symposium II, Part 2, 17 (May 1952).

5. R. M. Howe, Propagation of Underwater Sound in a Bilinear Velocity Gradient, AIR-3 (March 1953), University of Michigan Engineering Research Institute, ONR Contract N6 onr 23223; March, 1953.

6. Haneman and Howe, Solution of Partial Differential Equations by Difference Methods Using the Electronic Differential Analyzer, AIR-1 (October 1951), University of Michigan Engineering Research Institute.

7. Haneman and Howe, Solution of Partial Differential Equations by Difference Methods Using the Electronic Differential Analyzer, Proc. IRE., Vol. 40, pp. 1497-1508; October, 1952.

8. Timoshenko, Vibration Problems in Engineering, D. Van Nostrand (1937).

BIBLIOGRAPHY (continued)

9. Manley, Fundamentals of Vibration Study, Chapman and Hall, Ltd. (1948).

10. Korn and Korn, Electronic Analog Computers, McGraw-Hill (1952).

11. R. M. Howe, Electronic Differential Analyzer Solution of Beams with Nonlinear Damping, Report AIR-8, University of Michigan Engineering Research Institute, OOR Contract No. DA-20-018-ORD-21811; February, 1954.

12. R. M. Howe, Theory and Operating Instructions for the Air Comp Mod 4 Electronic Differential Analyzer, Report AIR-4, University of Michigan Engineering Research Institute, ONR Contract N6 onr 23223; March, 1953.

13. Williams, Amey, and McAdam, Wide-Band D-C Amplifier Stabilized for Gain and for Zero, Elec. Eng. 68, 934 (1949).

14. Lord Raleigh, Theory of Sound, Dover Publications (1945)

15. McCann and MacNeal, Beam-Vibration Analysis with the Electric-Analog Computer, Jour. of Applied Mechanics 17 (March 1950).